Design, Synthesis and Biological Evaluation of 3-Substituted-2-Oxindole Hybrid Derivatives as Novel Anticancer Agents

Romeo Romagnoli*[a], Pier Giovanni Baraldi[a], Filippo Prencipe[a], Paola Oliva[a], Stefania Baraldi[a], Maria Kimatrai Salvador[b], Luisa Carlota Lopez-Cara[b], Roberta Bortolozzi[c], Elena Mattiuzzo[c], Giuseppe Basso[c] and Giampietro Viola*[c]

[a]Dipartimento di Scienze Chimiche e Farmaceutiche, Università di Ferrara, 44121 Ferrara, Italy;

[b]Departamento de Química Farmaceútica y Orgánica Facultad de Farmacia, Campus de Cartuja s/n, 18071, Granada, Spain;

[c]Dipartimento di Salute della Donna e del Bambino, Laboratorio di Oncoematologia, Università di Padova, 35131 Padova, Italy

* To whom correspondence should be addressed. E-mail:rmr@unife.it; Phone: 39-(0)532-455303. Fax: 39-(0)532-455953. (R.R.); E-mail:giampietro.viola.1@unipd.it Phone: 39-(0)49-8215485. Fax: 39-(0)49-8211462. (G.V.).

Abstract: The 2-oxindole nucleus is the central core to develop new anticancer agents and its substitution at the 3-position can effect antitumor activity. Utilizing a pharmacophore hybridization approach, a novel series of antiproliferative agents was obtained by the modification of the structure of 3-substituted-2-oxindole pharmacophore by the attachment of the α-bromoacryloyl moiety, acting as a Michael acceptor, at the 5-position of 2-oxindole framework. The impact of the substituent at the 3-position of 2-oxindole core on the potency and selectivity against a panel of seven different cancer cell lines was examined. We found that these hybrid molecules displayed potent antiproliferative activity against a panel of four cancer cell lines, with one- to double digit nanomolar 50% inhibitory concentrations (IC_{50}). A distinctive selective antiproliferative activity was obtained towards CCRF-CEM and RS4;11 leukemic cell lines. In order to study the possible mechanism of action, we observed that the two most active compounds namely **3**(*E*) and **6**(*Z*) strongly induce apoptosis that follow the mitochondrial pathway. Interestingly a decrease of intracellular reduced glutathione content (GSH) and reactive oxygen species (ROS) production was detected in treated cells compared with controls suggesting that these effects may be involved in their mechanism of action.

Keywords. 2-Oxindole derivatives, α-bromoacryloyl, Michael acceptor, *in vitro* antiproliferative activity, GSH depletion.

1. Introduction

The 2-oxindole nucleus is a promising pharmacophore present in a wide series of compounds endowed of interesting biological properties as anticancer agents [1-7]. The fascinating properties of molecules bearing the 3-substituted-2-oxindole scaffold has attracted the attention of numerous researchers and 2-oxindole conjugates with heterocycles such as pyrrole and thiophene have been recognized as antineoplastic agents with a broad spectrum of activity against many cancer cell lines [8-10]. A wide number of 3-[(substituted-1*H*-pyrrol-2-yl)methylidenyl]-2-oxindole derivatives, such as SU 5402 (**1a**), SU 5416 or Semaxinib (**1b**),

SU 6668 (**1c**) and Sunitinib (**1d**) [11], have demonstrated promising antitumor activity and identified as receptor tyrosine kinase (RTK) inhibitors (Chart 1) [12]. By the modification of Sunitinib, Henise and Tauton identified an irreversible Never in mitosis gene A related Kinase 2 (Nek2) inhibitor (IC_{50}: 920 nM) through the introduction of the electrophilic propiolamide moiety at the 5-position of 2-oxindole ring (compound **1e**) [13a]. Analysis of the crystal structure of Nek2 in complex with Sunitinib-like derivatives revealed that the 5-position of the 2-oxindole nucleus was located in close proximity to Cys22 within the kinase [13b], such that the Michael acceptor moiety might covalently interact with the residue.

Noteworthy, the oxindole in the central nucleus of different Akt pathway inhibitors [7]. Nesi et al. have reported a series of 3,5-disubstituted-2-oxindole derivatives, in which the presence of the thiophene ring characterized the most active compound of the series. The 3-[(thiophen-2-yl)methylidenyl]-2-oxindole analogue **1f** was identified as an inhibitor of Akt phosphorylation and inhibited A549 cell proliferation with an IC_{50} of 0.66 μM [14].

The α-bromoacrylic acid is an alkylating moiety of low chemical reactivity and devoid of cytotoxic effects (IC_{50}>120 μM against murine leukemia L1210 cells) [15]. The α-bromoacryloyl moiety has provided the inspiration for the design and development of several covalently acting synthetic compounds. This chemical function was present in a series of potent anticancer distamycin-like minor groove binders, including PNU-166196 (brostallicin, compound **2**), which was evaluated as first-line single agent chemotherapy in patients with advanced or metastatic soft tissue sarcoma [16, 17]. Nowadays the research is primarily focused on the usage of brostallicin in combination with other chemotherapeutic drugs to target triple-negative breast cancer [18]. Regarding the chemical reactivity of the α-bromoacrylic moiety, we speculated that an intracellular biological nucleophile could perform a first-step Michael attack on the double bond, possibly followed by a further reaction of the alpha halogen to the carbonyl, leading to a beta-elimination or a second nucleophilic substitution [15]. Several findings suggest that GSH levels affect the antitumor activity of

brostallicin, supporting the hypothesis concerning the ability of brostallicin to react with GSH, giving a reactive compound able to bind DNA [19].

The most common class of reactive functional groups for selective alkylation of cysteine residues within the ATP-binding domain of their kinase targets are Michael acceptors [20]. In view of the importance of 3-substituted-2-oxindole as privileged structures for the preparation of anticancer agents [21-24], we decided to explore the synthesis and biological evaluation of novel molecular conjugates reported for the first time and obtained by the structural modification of 3-substituted-2-oxindole framework through the insertion at its 5-position of the α-bromoacryloylamido moiety, as a potential site of alkylation with a nucleophilic aminoacid residue within the kinase or with cellular nucleophiles such as glutathione. All hybrid molecules were characterized by a common 5-α-bromoacryloylamido-2-oxindole skeleton, anchored at its 3-position with two different heterocycles (pyrrole and thiophene) by an exocyclic double bond, to furnish pyrrol-2-yl [**3**(***Z***)], 2'-thienyl [**4**(***Z***) and **4**(***E***)], 3'-thienyl [**5**(***Z***) and **5**(***E***)], the isomeric 3'-methylthien-2'-yl [**6**(***Z***) and **6**(***E***)] and 5'-methylthien-2'-yl [**7**(***Z***) and **7**(***E***)] derivatives reported in the Chart 2. For compound **3**, the *Z*-form was favored due to the presence of an intramolecular hydrogen bond between the proton at *N*-1 position of pyrrole ring and the oxygen atom of the carbonyl group at the C-2 position of 2-oxindole core [12]. For all compounds (**4-7**) with thiophene ring at the 3-position of 2-oxindole nucleus, the two *E* and *Z* isomers were obtained and separated by flash chromatography. For derivatives **4** and **5**, the 3-exocyclic double bond was linked at the 2'- and 3'-position of thiophene ring, respectively, while analogues **6** and **7** were characterized by the presence of a methyl group at the 3'- and 5'-position, respectively, of the thiophen-2-yl moiety. This study deals with (a) the Structure-Activity Relationship (SAR) of the hybrid compounds **3-7** against a panel of seven different human cancer cells, (b) characterization of the mechanism of action through their evaluation of Nek2 inhibitory activity, (c) exploration of the effects induced by selected lead-compounds **3**(*Z*) and **6**(*E*) on apoptosis, mithocondrial depolarization and caspase-9 activation

and finally (d) capability of derivatives **3**(*Z*) and **6**(*E*) to induce depletion of glutathione (GSH) as well as Reactive Oxygen Species (ROS) production.

2. Chemistry

The designed 5-α-bromoacryloylamido-3-substituted indolin-2-one derivatives **3-7** were synthesized according to the procedure reported in Scheme 1. 5-Nitro-3-substituted-2-oxindole derivatives **8-12** were prepared by the Knoevenagel aldolic condensation between an equimolar mixture of the appropriate aldehyde with 5-nitro-2-oxindole in DMF at 80 °C in the presence of a catalytic amount of piperidine [9]. The pyrrole analogue **8** and the 2'-thienyl derivatives **9**, **11** and **12** existed exclusively as thermodynamically stable *Z*-isomer forms at the C-3 exocyclic double bond, while the thien-3'-yl derivative **10** (as a product of condensation with thiophen-3-carboxaldehyde) was isolated as a mixture of *Z* and *E* isomers. The 5-amino-2-oxindole derivatives **13-17** were generated starting from the corresponding analogues **8-12** by reduction of the nitro group with iron and ammonium chloride in a refluxing mixture of water and ethanol (1:4, v/v). While for the pyrrole derivative **8**, the corresponding amino analogues **13** was isolated exclusively in the *Z* configuration, the pure *Z* isomers of nitro derivatives **9**, **11** and **12** with 2-thienyl ring undergo partial isomerization to *E* isomers during the reduction of the nitro group and the related amino analogues **14**, **16** and **17**, respectively, were obtained as an inseparable mixture of both *Z* and *E* isomer forms. The 5-amino-2-oxindole derivatives **13-18** were converted to the hybrid compounds **3-7** and **19** by condensation with α-bromoacrylic acid using 1-ethyl-3-[3-(dimethylamino)propyl]carbodiimide hydrochloride (EDCI) in dimethylformamide.

For hybrid molecules **4-7**, the *E*/*Z* isomers were separated by silica gel flash chromatography and the configuration of the exocyclic double bond at the 3-position of the 2-oxindole core was assigned on results of NMR COSY and NOESY experiments. In general, *Z*-configurated compounds showed a strong interaction (NOE effect) between the vinylic proton and the hydrogen at the C-4 position of the 2-oxindole ring, while this effect was not observed for the

E-configurated compounds. For these latter isomers, a NOE effect was observed between the proton at the C-4 position of the benzene portion of the 2-oxindole nucleus and the proton(s) or methyl on the thiophene ring.

3. Biological results and discussion.

3.1. In vitro antiproliferative activities.

Table 1 summarizes the antiproliferative effects of the novel series of 5-α-bromoacryloylamido-3-substituted-2-oxindole derivatives **3-7** against the proliferation of a panel of seven different human cancer cells, using the propiolamide analogue **1e** and the 5-(α-bromoacryloylamido)-2-oxindole derivative **19** as reference compounds. We found that most of the new hybrid compounds displayed high antiproliferative activity towards a panel of seven cancer cell lines, with one-digit to double-digit nanomolar IC_{50} values. In general, the two leukemia cell lines CCRF-CEM and RS4;11 were the most sensitive to the influence of conjugates **3-7**, with compounds **3**(*Z*), **6**(*Z*) and **6**(*E*) which were active in the single-digit nanomolar range. Both the amino derivatives **13**(*Z*) and **15**(*E*/*Z*) did not exhibit tumor cell growth inhibitory activity (IC_{50}>10 μM), indicating that the α-bromoacryloyl moiety was essential for the antiproliferative effects of related compounds **3**(*Z*) and **4**(*Z*), respectively, confirming the validity of molecular hybridization approach. The 3'-methylthien-2'-yl derivative **6** with *Z*-configuration [**6**(*Z*)] resulted the most active compound of the series against CCRF-CEM, RS4;11 and HeLa, with IC_{50} values of 0.5, 0.4 and 420 nM, respectively, resulting equipotent with the unsubstituted thien-2'-yl and 5'-methylthien-2'-yl analogues **4**(*E*) and **7**(*E*), respectively, against HL-60 cells.

Based on the biological data reported in the Table 1, many structure-activity relationships (SARs) could be deduced. We have found that the potency and selectivity of hybrid compounds **3-7** against the different cancer cell lines depends on the substituent and

configuration of the double bond at the C-3 position of the 2-oxindole core, with the *E*- and *Z*-isomers which displayed different antiproliferative activities.

This suggests that the pyrrole substituent at the 3-position of 2-oxindole system was favourable for antiproliferative activity. The pyrrole derivative **3**(*Z*) resulted considerably more potent against CCRF-CEM and RS4;11 cells, with IC_{50} values in the single digit nanomolar range. The comparison between the two pyrrole derivatives **1e** and **3**(*Z*) revealed different potency trends depending on the electrophile at the 5-position of the 2-oxindole core. Thus, the propinamide derivative **1e** resulted from 3- to 70-fold less potent than the α-bromoacryloylamido counterpart **3**(*Z*). The reduction of activity was more evident against HL-60 and RS4;11 cell lines, with a 41- and 70-fold reduction of potency, respectively. By comparison of compounds **8**(*Z*) and **3**(*Z*), the electrophilic α-bromoacryloyl moiety was essential for a potent antiproliferative activity, as revealed by the sharply reduced activity of the corresponding amino derivative **8**(*Z*).

The 5-(α-bromoacryloylamido)-2-oxindole derivative **19** was from 2- to 220-fold less potent than the corresponding 3-((*1H*-pyrrol-2'-yl)methylene) hybrid conjugate **3**(*Z*). This data suggests that the hybridization of compound **19** with pyrrole-2-methylene unit, to generate **3**(*Z*), lead to an enhanced antiproliferative activity and further validate the concept that anticancer activity can be increased by the hybridization of two different pharmacophoric functional groups.

With the exception of HT-29 cells, the bioisosteric replacement of pyrrole with 2'-thiophene [compounds **3**(*Z*) and **4**(*Z*), respectively] decreased potency from 1.5- to 12-fold compared with **3**(*Z*) on six of the seven cancer cell lines, indicating that pyrrole and thiophene are not bioequivalent at the 3-position of the 2-oxindole ring. For the 2'-thienyl derivative **4**, *E*-isomer showed improved antiproliferative activity with respect to the *Z*-form against HL-60, Jurkat and CCRF-CEM cell lines, with IC_{50} values of 15, 16 and 10 nM, respectively, while the potency was reduced on RS4;11, HT-29 and MCF-7 cancer cells. The *E* and *Z* isomers

were equipotent on HeLa cells. Comparing the two regioisomeric thiophene derivatives **4** and **5**, in general the 2'-thienyl derivatives were more potent the 3'-thienyl counterpart [**4**(*Z*) *vs.* **5**(*Z*) and **4**(*E*) *vs.* **5**(*E*)]. In comparing the two isomeric forms of the thien-3'-yl derivative **5** with each other, there was only minor difference in IC_{50} values against CCRF-CEM, RS4;11, HeLa and MCF-7 cells, except than *Z*-isomer was 2-fold more active against the HL-60 cells, while the *E*-isomer was 3-, 1.5- and 2- fold more active against Jurkat, HeLa and HT-29 cells. For the thien-3'-yl derivative **5**, comparing the *Z*- with the *E*-isomeric form, the latter was more active against Jurkat and HT-29 cells, in contrast *Z*-isomer was 2-fold more active than *E*-isomer in HL-60 and HT-29 cells, while the two compounds were equipotent against RS4;11, HeLa and MCF-7 cells.

The data reported in the Table 1 indicated that substitution changes in the thiophene at the 3-position of 2-oxindole nucleus triggered significantly changes in the antiproliferative activity. Comparing compounds which shared common geometry at the 3-exocyclic double bond [**4**(*Z*) and **5**(*Z*) *vs.* **6**(*Z*) and **7**(*Z*), **4**(*E*) and **5**(*E*) *vs.* **6**(*E*) and **7**(*E*), in general, the introduction of the small methyl group at the 3'- or 5'-position of the thophene ring improved significantly the antiproliferative activity, with single digit nanomolar activity against CCRF-CEM cells. The contribution of the methyl group on thiophene ring to activity [**6**(*Z*) *vs.* **7**(*Z*), **6**(*E*) *vs.* **7**(*E*)] was position dependent.

For the *Z*-isomer of 3'-methylthiophen-2'-yl derivative **6**, moving the methyl group from the 3'- to the 5'- position, to furnish derivative **7**(*Z*), resulted in 1.5- to 125-fold of reduction in antiproliferative activity against five of the seven cancer cell lines, while the two compounds were equipotent against MCF-7 cells, but compound **7**(*Z*) was 2-fold more active than **6**(*Z*) against HT-29 cells. By comparison of the two derivatives **6** and **7** which shared common *E*-geometry at the exocyclic double bond, the 3'-methyl derivative **6** was from 4- to 5-fold less potent than 5'-methyl counterpart **7** on four of the seven cancer cell lines, while the two

compounds were equipotent against CCRF-CEM and HT-29 cells. Only in HL-60 cells, compound **7** was 3-fold more potent than **6**.

Compound **7**(*Z*) was from 2- to 9-fold fold less active than the corresponding *E*-isomer against five of the seven cancer cell lines, while the difference between *E* and *Z*-form was minimal in HeLa cells. Only in MCF-7 cells, *Z*-isomer was more potent than *E*-isomer (IC_{50} 3 and 4.4 μM). An opposite effect was observed for the regioisomeric 3'-methylthiophen-2'-yl derivative **6**, where the *Z*-isomeric form had greater potency (from 1.5- to 10-fold) than compound with *E* configuration against HL-60, Jurkat, CCRF-CEM and RS4;11 cells, comparable activity against HeLa and MCF-7 cells and less activity against HT-29 cells. Derivative **6**(*Z*) exhibited potent activity, with subnanomolar IC_{50} values against both the CCRF-CEM and RS4;11 cell lines.

Comparing the *E*-isomers of 3'- and 5'-methythiophen-2'-yl derivatives **6** and **7**, the 3'-methyl derivative **6**(*E*) was 3-5-fold less active than 5'-methyl analogue **7**(*E*) against HL-60 cells, with a minimal difference in potency between the two derivatives in the CCRF-CEM, MCF-7 and HT-29 cells, while **6**(*E*) was more potent than **7**(*E*) against Jurkat, RS4;11 and HeLa cells. With the exception of HeLa, HT-29 and MCF-7 cancer cells, compounds **4**(*E*), **6**(*Z*) and **6**(*E*) were the most active derivatives in the series of thiophene analogues **4-7**, exhibiting IC_{50} values in the single or double-digit nanomolar range against four of the seven cancer cell lines. With the exception of both the isomeric forms of thien-3'-yl derivative all the conjugates prepared were more active than the reference compound **1e**.

This study suggested that the two key pharmacophoric elements, namely the α-bromoacryloyl amido and the heterocycle as well as the configuration of the double bond at the 5- and 3-positions of 2-oxindole skeleton are important to achieve potent antiproliferative agents.

*3.2 Cytotoxicity of compounds **3**(Z) and **6**(E) in peripheral blood lymphocytes (PBL)*

To obtain a preliminary indication of the cytotoxic potential of these derivatives in normal human cells, two of the most active compounds [**3**(*Z*) and **6**(*E*)] were evaluated *in vitro* against peripheral blood lymphocytes (PBL) from healthy donors. Compounds **3**(*E*) and **6**(*Z*) showed an IC_{50} of 1.5 μM and 0.45 μM respectively, in quiescent lymphocytes (Table 2), whereas in lymphocytes in an active phase of proliferation induced by phytohematoagglutinin (PHA) a mitogenic stimulus showed similar results having an IC_{50} of 0.85 and 1.22 μM respectively. Anyway these values are higher than that observed against Jurkat and CCRF-CEM lymphoblastic cell lines and the results indicate that these compounds have low toxicity in normal cells in comparison to tumor cells, suggesting a potential for a good therapeutic index.

3.3 Evaluation of Nek2 inhibitory activity

Since the introduction of the electrophilic propargylamide moiety at the 5-position of 2-oxindole ring (**1e**) produce compounds able to inhibit Nek2 [13a], we evaluated if also our new derivatives were able to inhibit the enzyme. As reference compound **1e** was also runned.

As depicted in Figure 1 (panel A, the enzymatic activity evaluated in the presence of test compounds at the concentration of 1 μM, is reduced by about 50% only in the presence of compound **3**(*Z*) and in well agreement with previous work also by **1e** [13a], while all the other derivatives present a weak activity (5-20% inhibition). These results suggest that apart compound **3**(*Z*) in which a inhibition of the enzymatic activity is conserved, although lower respect to compound **1e**, the introduction of the α-bromoacryloyl mojety causes the disappearance of the inhibitory activity on the kinase.

In addition we also evaluated if the test compounds induce variation of the cell cycle in particular if they are able to delay mitotic exit. As showed in Figure 1 (Panel B) two of the most active antiproliferative compounds [**3**(*Z*) and **6**(*E*)] were analyzed after 24 h of treatment in Hela cells. The result indicate that both compounds along with the reference compound **1e**

induce only slight variation of the cell cycle. In particular a decrease of G1 phase of about 20% was observed for compounds **3**(*Z*) and **6**(*E*) at the highest concentration used (1 μM), while the reference compound **1e** do not show any significant variations.

*3.4 Compounds **3**(E) and **6**(Z) induce apoptosis in both Jurkat and Hela cells*

With the purpose to investigate the mode of cell death induced by the new derivatives the annexin-V assay was used in both HeLa and Jurkat cells treated with compounds **3**(*Z*) and **6**(*E*) at different concentrations. As depicted in Figure 2, HeLa cells (Panels A and B), treated with the two compounds at the concentration of 0.5 and 1 μM for 24 h or 48 h showed an accumulation of annexin-V positive cells in comparison with the control, in a concentration and time-dependent manner, and this is indicative of the occurrence of apoptosis. In well agreement with the antiproliferative potency found in leukemic cells, both compounds induce apoptosis in Jurkat cells (Panels C and D) but at concentration ten fold lower (100 nM) than that used in HeLa cells.

*3.5 Compounds **3**(E) and **6**(Z) induce mitochondrial depolarization and caspase-9 activation in Hela cells*

It is well known that an event recognized to be important in apoptosis is the depolarization of mitochondrial membrane due to mitochondrial permeability transition (MPT) [25, 26]. Thus, we determined whether **3**(*E*) and **6**(*Z*) induced an alteration of the mitochondrial transmembrane potential ($\Delta\psi_{mt}$). $\Delta\psi_{mt}$ was monitored by flow cytometry using the dye 5,5',6,6'-tetrachloro-1,1',3,3'-tetraethylbenzimidazolcarbocyanine (JC-1) [27]. As showed in Figure 3 (Panels A and B), the two compounds induce a significant depolarization starting after 12-24 h of treatment indicative of mitochondrial pore opening. In particular the effect is more evident in HeLa (panel A) cells respect to Jurkat (panel B), although in these last we observed a marked depolarization already after 12 h of treatment.

To further study the apoptotic pathway we analyzed the cleavage of caspase-9 an effector caspase involved in inducing mitochondrial damage during apoptosis [28]. As showed in Figure 3 (panel C) in HeLa cells treated with the two compounds, we observed the appearance of cleaved fragment suggesting activation of caspase-9.

*3.6 Compounds **3**(E) and **6**(Z) induce ROS production and GSH depletion*

To better understand the mechanism of action of the test compounds, we analyzed if they induce ROS production. Both HeLa and Jurkat cells were treated for 12 h and 24 h with **3**(*E*) and **6**(*Z*), and the levels of intracellular ROS were monitored by flow cytometry with the fluorescent probes, 2',7'-dichlorodihydrofluorescein diacetate (H_2DCFDA) [29]. As shown in Figure 4 (panels A and B), flow cytometric analysis showed a modest increase in the DCF-positive cells, in the first times of treatment, but increase later with time in a manner similar to what was observed with the mitochondrial potential. In particular the two compounds do not present significant differences between them. Given that the mitochondrial membrane depolarization has been associated with mitochondrial production of ROS [30,31], these findings suggest that ROS, detected by H_2DCFDA, could be produced as a consequence of mitochondrial damage.

Since it is well known the chemical reactivity of the α-bromoacrylic moiety toward biological nucleophiles including reduced glutathione (GSH) [17,32,33], we determined whether these compounds caused a decrease in intracellular GSH content. Therefore, we analyzed HeLa and Jurkat cells for changes in their GSH levels, by flow cytometry using the fluorescent probe 5-chloromethylfluorescein diacetate (CMFDA) [34]. As shown in Figure 4 (Panels C and D), incubations with either **3**(*Z*) or **6**(*E*) for 12 h and 24 h, reduced CMFDA fluorescence, in both cell lines indicating GSH depletion.

Although intracellular GSH loss is an early feature in the progression of cell death in response to different apoptotic stimuli and because of its action as a primary intracellular antioxidant in the cells, a reduction in intracellular GSH content is generally believed to reflect generation of

ROS [35]. Thus, to prove that ROS are involved in the mechanism of cell death of compounds **3**(*Z*) and **6**(*E*) we analyzed cell viability in the presence of tocopherol acetate (TOC), and N-acetylcysteine (NAC), two well known antioxidant. As shown in Figure 5 NAC, but not TOC significantly protected HeLa cells from the antiproliferative effect of the two compounds increasing cell viability. This suggests that ROS may be involved in the antiproliferative effects observed with **3**(*Z*) and **6**(*E*).

We also investigated whether **3**(*Z*) and **6**(*E*) may induce DNA damage by examining the expression of phosphorylated histone H2AX at Ser139 (γH2A.X) upon treatment in HeLa cells. γH2A.X phosphorylation occurs after DNA double strand break (DSB) induction, thus identifying γH2A.X as an early sensitive indicator of DSBs [36]. As shown in Figure 5, after a 24 h treatment both compounds induced γH2A.X expression indicating that they induced DNA damage probably by oxidative stress.

4. Conclusions

Molecular hybridization, which covalently combines two pharmacophores in a single molecule, is an effective tool to design highly active novel entities. The α-bromoacryloyl moiety is an efficient and versatile electrophilic warhead that can be combined with a recognition moiety to address specific enzymatic target. Several laboratories reported that the 2-oxindole is one of the most effective and newly emerging scaffold that has been frequently used as pharmacophore to generate molecules that possesses anticancer activity against various human tumor cell lines. In this context and in continuation of our previous works, the insertion of a α-bromoacryloyl moiety at the 5-position of the 3-substituted-2-oxindole framework allowed a higher number of sequential interactions with cellular nucleophiles which contribute significantly to the increased antiproliferative activity showed by these hybrid molecules. The structure-activity relationship study highlights the importance of generate hybrid structures from these two pharmacophores, where biological activity was achieved due to the effect of each entity in the unique structure resulted of the molecular

hybridization. Our findings indicate the importance of substituent at the 3-position of 2-oxindole skeleton for activity and selectivity against different cancer cell lines. In general, there was a trend that the antiproliferative activities of conjugates **3-7** were somewhat more pronounced against HL-60, Jurkat, CCRF-CEM and RS4;11 as compared with HeLa, HT-29 and MCF-7 cancer cells. Specific effects seemed to vary with the cell line tested. Thus, compounds **4**(*E*), **6**(*Z*) and **7**(*E*) had the greatest activity on HL-60 cells, **4**(*E*) with Jurkat cells, **6**(*Z*) with CCRF-CEM, RS4;11 and HeLa cells, **4**(*Z*) with HT-29 cells and **3**(*Z*) with MCF-7.

Comparing the antiproliferative activities of compounds **1e** and **3**(*Z*), the propiolamide moiety was less efficacious than the α-bromoacryloylamido group as electrophile with biological nucleophiles. Importantly, **1e** is an irreversible inhibitor of the Nek2 kinase, whereas **3**(Z) is endowed with lower activity in the enzymatic activity. Thus while the insertion of the α-bromoacryloyl moiety dramatically reduced the inhibitory activity on this enzyme at the same time significantly increase the cell growth inhibitory activity.

Preliminary studies devoted to the elucidation of mechanism of action demonstrated that the most potent hybrid compounds strongly induce apoptosis that follows the mitochondrial pathway, as demonstrated by mitochondrial depolarization and caspase-9 cleavage. More precisely their activity seems to be related to depletion of intracellular GSH and consequent imbalance in the antioxidant defense of the cells that lead to ROS production [37]. If intracellular GSH depletion occur through a direct chemical reaction or through interfering with the enzymatic synthesis of GSH remains to be determined. Considering that human tumors often show increased GSH content compared to normal tissues, the interaction of compounds **3**(*E*) and **6**(*Z*) with glutathione suggest that these molecules may have a potential value for the treatment of cancers characterized by constitutive or therapy-induced overexpression of glutathione/glutathione-S-tranferase (GST) levels. The potent anticancer activity and synthetic accessibility strongly encourage further optimization of hybrid

compound **3**(*Z*) as lead to develop more potent irreversible Nek2 kinase inhibitors. Further, we believe that with interesting *in vivo* activity this series of new molecules is important and should be pursued.

5. Experimental protocols

5.1. Chemistry

5.1.1. Materials and Methods

^{1}H experiments were recorded on either a Bruker AC 200 or a Varian 400 Mercury Plus spectrometer, while ^{13}C NMR spectra were recorded on Varian 400 Mercury Plus spectrometer. Chemical shifts (δ) are given in ppm upfield from tetramethylsilane as internal standard, and the spectra were recorded in appropriate deuterated solvents, as indicated. Positive-ion electrospray ionization (ESI) mass spectra were recorded on a double-focusing Finnigan MAT 95 instrument with BE geometry. Melting points (mp) were determined on a Buchi-Tottoli apparatus and are uncorrected. All products reported showed ^{1}H and ^{13}C NMR spectra in agreement with the assigned structures. The purity of tested compounds was determined by combustion elemental analyses conducted by the Microanalytical Laboratory of the Chemistry Department of the University of Ferrara with a Yanagimoto MT-5 CHN recorder elemental analyzer. All tested compounds yielded data consistent with a purity of at least 95% as compared with the theoretical values. Standard syringe techniques were used for transferring dry solvents. Reaction courses and product mixtures were routinely monitored by TLC on silica gel (precoated F_{254} Merck plates), and compounds were visualized with aqueous $KMnO_4$. Flash chromatography was performed using 230-400 mesh silica gel and the indicated solvent system. Organic solutions were dried over anhydrous Na_2SO_4.

*5.1.2. General procedure A for the synthesis of compounds **8-12**.*

A reaction mixture of 5-nitroindolin-2-one (356 mg, 2 mmol), the appropriate aldehyde (2.4 mmol, 1.2 equiv.) and piperidine (21 μL, 0.2 mmol, 0.1 equiv,) in DMF (5 mL) was stirred at 80 °C for 4h. The solvent was removed under reduced pressure, the resulting residue was suspended in ethyl ether (15 mL) and filtered, to furnish the target compound used without any further purification for the next reaction.

*5.1.2.1. (Z)-3-((1H-pyrrol-2-yl)methylene)-5-nitroindolin-2-one **(8)**.* Following general procedure A, compound **8**(*Z*) was isolated as a brown solid. Yield: 91%, mp 184-186 ºC. ^{1}H-NMR (200 MHz, d_6-DMSO) δ: 6.43 (m, 1H), 6.97 (m, 1H), 7.03 (d, *J*=8.8 Hz, 1H), 7.47 (m, 1H), 8.06 (dd, *J*=8.8 and 2.6 Hz, 1H), 8.17 (s, 1H), 8.59 (d, *J*=2.2 Hz, 1H), 11.2 (bs, 1H), 13.15 (s, 1H). MS (ESI): $[M+1]^+$=256.2.

*5.1.2.2. (Z)-5-Nitro-3-(thiophen-2-ylmethylene)indolin-2-one **(9)**.* Following general procedure A, compound **9**(*Z*) was obtained as a brown solid. Yield: >95%, mp 241-243 ºC. ^{1}H-NMR (200 MHz, d_6-DMSO) δ: 7.01 (m, 1H), 7.03 (d, *J*=8.8 Hz, 1H), 7.47 (m, 1H), 8.03 (m, 2H), 8.17 (dd, *J*=8.8 and 2.4 Hz, 1H), 8.56 (s, 1H), 8.66 (d, *J*=2.2 Hz, 1H), 11.2 (bs, 1H). MS (ESI): $[M+1]^+$=273.3.

*5.1.2.3. (Z)-and (E) isomer mixture of 5-nitro-3-(thiophen-3-ylmethylene)indolin-2-one **(10)**.* Following general procedure A, compound **10** (*E*/*Z* mixture) were obtained as a brown solid. Yield: >95%, mp 226-232 ºC. ^{1}H-NMR (200 MHz, d_6-DMSO) δ: 6.99 (d, *J*=8.8 Hz, 1H), 7.01 (m, 1H), 7.08 (d, *J*=8.8 Hz, 1H), 7.47 (m, 1H), 7.67 (m, 2H), 7.84 (m, 2H), 8.12 (m, 2H), 8.18 (s, 1H), 8.28 (s, 1H), 8.51 (d, *J*=2.2 Hz, 1H), 8.65 (d, *J*=2.2 Hz, 1H), 11.3 (bs, 2H). MS (ESI): $[M+1]^+$=273.4.

*5.1.2.4. (Z)-3-((3-Methylthiophen-2-yl)methylene)-5-nitroindolin-2-one **(11)**.* Following general procedure A, compound **11**(*Z*) was obtained as a brown solid. Yield: 91%, mp 283 ºC.

^{1}H-NMR (200 MHz, d_6-DMSO) δ: 2.58 (s, 3H), 7.01 (d, *J*=8.6 Hz, 1H), 7.09 (d, *J*=5.0 Hz, 1H), 7.87 (d, *J*=5.0 Hz, 1H), 8.09 (dd, *J*=8.6 and 2.2 Hz, 1H), 8.24 (s, 1H), 8.82 (d, *J*=2.2 Hz, 1H), 10.8 (bs, 1H). MS (ESI): $[M+1]^+$=287.3.

*5.1.2.5. (Z)-3-((5-methylthiophen-2-yl)methylene)-5-nitroindolin-2-one (**12**).* Following general procedure A, compound **12**(*Z*) was obtained as a purple solid. Yield: 92%, mp 252-254 ºC. ^{1}H-NMR (200 MHz, d_6-DMSO) δ: 2.56 (s, 3H), 7.03 (m, 2H), 7.81 (d, J=4.0 Hz, 1H), 8.11 (dd, *J*=8.6 and 2.2 Hz, 1H), 8.62 (d, *J*=2.2 Hz, 1H), 8.62 (d, *J*=2.2 Hz, 1H), 11.2 (bs, 1H). MS (ESI): $[M+1]^+$=287.3.

*5.1.3. General procedure B for the synthesis of compounds **13-18**.*

To a suspension of 5-nitro-3-substituted-2-oxindole derivatives **8-12** or commercially available 5-nitroindolin-2-one (1 mmol) in a mixture of ethanol and water (10 mL, 4:1 v/v) was added iron powder (560 mg. 10 mmol, 10 equiv.) and NH_4Cl (134 mg, 2.5 mmol, 2.5 equiv.). The mixture was refluxed for 2 h, cooled and filtered through Celite. The filtrate was diluted with water (5 mL) and extracted with dichloromethane (3 x 10 mL). The combined organic layers were washed with water (10 mL) and brine (10 mL), dried over anhydrous Na_2SO_4 and concentrated under reduced pressure. The crude residue was purified by crystallization with ethyl ether**.**

*5.1.3.1. (Z)-3-((1H-pyrrol-2-yl)methylene)-5-aminoindolin-2-one (**13**).* Following general procedure B, compound **13**(*Z*) was isolated as a red solid. Yield: 58%, mp 148-150 ºC. ^{1}H-NMR (200 MHz, d_6-DMSO) δ: 4.66 (bs, 2H), 6.29 (m, 1H), 6.41 (dd, *J*=8.0 and 1.2 Hz, 1H), 6.54 (d, *J*=8.0 Hz, 1H), 6.79 (m, 2H), 7.28 (d, *J*=1.2 Hz, 1H), 7.44 (s, 1H), 10.4 (s, 1H), 13.4 (s, 1H). ^{13}C NMR (100 MHz, d_6-DMSO) δ: 168.97, 143.42, 129.97, 129.48, 125.70, 125.07, 124.96, 119.58, 118.09, 113.23, 111.09, 109.91, 104.74. MS (ESI): $[M+1]^+$=226.2.

*5.1.3.2. (Z) and (E) isomer mixture of 5-amino-3-(thiophen-2-ylmethylene)indolin-2-one (**14**).* Following general procedure B, the mixture of the two isomers (*Z*) and (*E*) was obtained as a brown solid. Yield: 65%, mp 180-182 ºC. ^{1}H-NMR (200 MHz, d_6-DMSO) δ: 4.70 (bs, 4H), 6.44 (d, *J*=8.0 Hz, 1H), 6.54 (m, 2H), 6.59 (d, *J*=8.0 Hz, 1H), 6.87 (s, 1H), 7.18 (t, *J*=2.0 Hz, 1H), 7.27 (t, *J*=2.0 Hz, 1H), 7.63 (d, *J*=1.4 Hz, 1H), 7.74 (d, *J*=1.4 Hz, 1H), 7.81 (bs, 2H), 7.87 (d, *J*=1.4 Hz, 1H), 7.95 (d, *J*=2.2 Hz, 1H), 8.01 (d, *J*=2.2 Hz, 1H), 10.1 (bs, 2H),. MS (ESI): $[M+1]^+$=243.3.

*5.1.3.3. (Z) and (E) isomer mixtutre of 5-amino-3-(thiophen-3-ylmethylene)indolin-2-one (**15**).* Following general procedure B, the mixture of the two isomers (*Z*) and (*E*) was obtained as a red solid. Yield: 58%, mp 64-66 ºC. ^{1}H-NMR (200 MHz, d_6-DMSO) δ: 4.75 (bs, 4H), 6.48 (m, 3H), 6.60 (d, *J*=8.0 Hz, 1H), 6.86 (d, *J*=1.4 Hz, 1H), 7.12 (d, *J*=2.0 Hz, 1H), 7.49 (d, J=8.0 Hz, 1H), 7.51 (s, 1H), 7.58 (m, 2H), 7.71 (dd, *J*=8.0 and 2.4 Hz, 1H), 8.06 (d, *J*=1.4 Hz, 1H), 8.09 (m, 1H), 8.80 (d, *J*=2.4 Hz, 1H),10.1 (bs, 1H), 10.2 (bs, 1H). MS (ESI): $[M+1]^+$=243.3.

*5.1.3.4. (Z) and (E) isomers of 5-amino-3-((3-methylthiophen-2-yl)methylene)indolin-2-one (**16**).* Following general procedure B, the mixture of the two isomers (*Z*) and (*E*) was obtained as a yellow oil. Yield: 62%. ^{1}H-NMR (200 MHz, d_6-DMSO) δ: 2.38 (s, 3H). 2.40 (s, 3H). 4.77 (bs, 4H), 6.52 (m, 4H), 6.96 (d, *J*=2.0 Hz, 1H), 7.05 (d, *J*=5.2 Hz, 1H), 7.14 (d, *J*=5.2 Hz, 1H), 7.49 (d, *J*=2.0 Hz, 1H), 7.63 (d, *J*=6.0 Hz, 2H), 7.71 (d, *J*=4.6 Hz, 1H), 7.84 (d, *J*=5.4 Hz, 1H), 10.1 (bs, 1H), 10.2 (s, 1H). MS (ESI): $[M+1]^+$=287.3.

*5.1.3.5. (Z) and (E) isomers of 5-amino-3-((5-methylthiophen-2-yl)methylene)indolin-2-one (**17**).* Following general procedure B, the mixture of the two isomers (*Z*) and (*E*) was obtained as a brown solid. Yield: 65%, mp 180-182 ºC. ^{1}H-NMR (200 MHz, d_6-DMSO) δ: 2.58 (s, 3H). 2.59 (s, 3H). 4.66 (bs, 2H), 4.80 (bs, 2H), 6.42 (d, *J*=2.0 Hz, 1H), 6.46 (d, *J*=2.0 Hz, 1H), 6.51 (m, 1H), 6.52 (d, *J*=3.4 Hz, 1H), 6.55 (d, *J*=3.4 Hz, 1H), 6.61 (s, 1H), 6.86 (d, *J*=3.4 Hz,

1H), 6.91 (dd, *J*=8.6 and 2.2 Hz, 1H), 7.02 (dd, *J*=8.6 and 2.2 Hz, 1H), 7.52 (d, *J*=3.4 Hz, 1H), 7.57 (dd, *J*=8.6 and 2.2 Hz, 1H), 7.70 (m, 1H), 10.1 (bs, 2H). MS (ESI): $[M+1]^+$=287.3.

*5.1.3.6. 5-Aminoindolin-2-one (**18**).* Following general procedure B, starting from the commercially available 5-nitroindolin-2-one, the corresponding 5-aminoindolin-2-one **18** was isolated as a brown solid. Yield: 78%, mp 137-138 ºC. ^{1}H-NMR (200 MHz, d_6-DMSO) δ: 3.31 (s, 2H). 4.75 (bs, 2H), 6.32 (dd, *J*=8.6 and 2.2 Hz, 1H), 6.48 (m, 2H), 9.93 (bs, 1H). MS (ESI): $[M+1]^+$=149.2.

*5.1.4. General procedure C for the synthesis of compounds **3-7** and **19**.*

To an ice-cooled solution of amino derivative **13-18** (1.00 mmol) in dry DMF (5.0 mL) were added a mixture of EDCI (383 mg, 2.00 mmol) and α-bromoacrylic acid (2.00 mmol, 306 mg). The reaction mixture was stirred at room temperature for 18 h and then concentrated under reduced pressure. The residue was dissolved with a mixture of CH_2Cl_2 (15 mL) and water (5 mL), and the organic phase was washed with brine (5 mL), dried over Na_2SO_4 and evaporated to dryness *in vacuo*. The resulting crude residue was purified by column chromatography on silica gel.

*5.1.4.1. (Z)-N-(3-((1H-pyrrol-2-yl)methylene)-2-oxoindolin-5-yl)-2-bromoacrylamide (**3**).* Following general procedure C, after workup as described previously, the residue was purified by flash chromatography on silica gel using light petroleum ether: EtOAc 1:1 as eluent, affording compound **3**(*Z*) as an orange solid. Yield: 56%, mp 219-221 ºC. ^{1}H-NMR (400 MHz, d_6-DMSO) δ: 6.29 (d, *J*=3.2 Hz, 1H), 6.35 (dd, *J*=1.8 and 1.2 Hz, 1H), 6.75 (d, *J*=3.2 Hz, 1H), 6.84 (d, *J*=8.4 Hz, 1H), 6.90 (d, *J*=1.8 Hz, 1H), 7.27 (dd, *J*=8.4 and 2.0 Hz, 1H), 7.37 (d, *J*=1.2 Hz, 1H), 7.66 (s, 1H), 7.92 (d, *J*=2.0 Hz, 1H), 10.1 (s, 1H), 10.9 (s, 1H), 13.3 (s, 1H). ^{13}C NMR (100 MHz, d_6-DMSO) δ: 109.30, 111.40, 111.97, 116.52, 120.25, 120.75, 125.07, 125.18, 125.48, 125.87, 126.39, 129.39, 132.02, 135.74, 160.59, 169.21. MS

(ESI): $[M]^+$=358.09, $[M+2]^+$=360.20. Anal. ($C_{16}H_{12}BrN_3O_2$) C, H, N. Anal. calcd for $C_{16}H_{12}BrN_3O_2$. C, 53.65; H, 3.38; N, 11.73; found: C, 53.48; H, 3.21; N, 11.58.

*5.1.4.2. (Z)-2-Bromo-N-(2-oxo-3-(thiophen-2-ylmethylene)indolin-5-yl)acrylamide (**4**) and (E)-2-bromo-N-(2-oxo-3-(thiophen-2-ylmethylene)indolin-5-yl)acrylamide (**4**).* Following general procedure C, after workup as described previously, the residue was purified by gradient flash chromatography on silica gel using EtOAc-light petroleum ether from 4:6 to 1:1 as eluent, affording compound **4**(*Z*) (EtOAc-light petroleum ether 4:6) and **4**(*E*) (EtOAc-light petroleum ether 1:1).

Compound 4(*Z*). Yellow solid. Yield: 43%, mp 186-188 ºC. ^{1}H-NMR (400 MHz, d_6-DMSO) δ: 6.29 (d, *J*=2.8 Hz, 1H), 6.76 (d, *J*=2.8 Hz, 1H), 6.82 (d, *J*=8.4 Hz, 1H), 7.22 (dd, *J*=5.2 and 3.6 Hz, 1H), 7.30 (dd, *J*=8.4 and 2.0 Hz, 1H), 7.89 (d, *J*=5.2 Hz, 1H), 7.97 (m, 2H), 8.05 (s, 1H), 10.2 (s, 1H), 10.6 (s, 1H). ^{13}C NMR (100 MHz, d_6-DMSO) δ: 109.25, 113.18, 121.39, 121.99, 124.23, 125.16, 125.59, 127.41, 128.45, 131.75, 134.63, 137.14, 137.30, 138.08, 160.64, 167.35. MS (ESI): $[M]^+$=375.19, $[M+2]^+$=377.17. Anal. calcd for $C_{16}H_{11}BrN_2O_2S$. C, 51.21; H, 2.95; N, 7.47; found: C, 51.03; H, 2.76; N, 7.35.

Compound 4(*E*)**.** Yellow solid. Yield: 21%, mp 167-169 ºC. ^{1}H-NMR (400 MHz, d_6-DMSO) δ: 6.29 (d, *J*=3.2 Hz, 1H), 6.73 (d, *J*=3.2 Hz, 1H), 6.87 (d, *J*=8.0 Hz, 1H), 7.32 (dd, *J*=5.2 and 3.6 Hz, 1H), 7.46 (dd, *J*=8.0 and 2.0 Hz, 1H), 7.79 (s, 1H), 7.83 (d, *J*=3.6 Hz, 1H), 8.05 (d, *J*=5.2 Hz, 1H), 8.64 (d, *J*=2.0 Hz, 1H), 10.3 (s, 1H), 10.6 (s, 1H). ^{13}C NMR (100 MHz, d_6-DMSO) δ: 109.68, 116.22, 120.58, 122.45, 123.24, 125.05, 125.54, 127.50, 128.69, 132.09, 132.35, 136.08, 136.98, 139.14, 160.82, 169.23. MS (ESI): $[M]^+$=375.31, $[M+2]^+$=377.17. Anal. calcd for $C_{16}H_{11}BrN_2O_2S$. C, 51.21; H, 2.95; N, 7.47; found: C, 50.98; H, 2.78; N, 7.28.

*5.1.4.3. (Z)-2-Bromo-N-(2-oxo-3-(thiophen-3-ylmethylene)indolin-5-yl)acrylamide (**5**) and (E)-2-bromo-N-(2-oxo-3-(thiophen-3-ylmethylene)indolin-5-yl)acrylamide (**5**).* Following general procedure C, after workup as described previously, the residue was purified by

gradient flash chromatography on silica gel using EtOAc-light petroleum ether from 4:6 to 1:1 as eluent, affording compound **5**(*Z*) (EtOAc-light petroleum ether 4:6) and **5**(*E*) (EtOAc-light petroleum ether 1:1).

Compound 5(*Z*)**.** Yellow solid. Yield: 24%, mp 204-206 ºC. ^{1}H-NMR (400 MHz, d_6-DMSO) δ: 6.29 (d, *J*=2.8 Hz, 1H), 6.75 (d, *J*=2.8 Hz, 1H), 6.80 (d, *J*=8.4 Hz, 1H), 7.31 (dd, *J*=8.0 and 2.0 Hz, 1H), 7.62 (dd, *J*=4.8 and 2.8 Hz, 1H), 7.78 (s, 1H), 7.95 (d, *J*=2.0 Hz, 1H), 8.15 (d, *J*=5.2 Hz, 1H), 8.86 (d, *J*=2.8 Hz, 1H), 10.2 (s, 1H), 10.6 (s, 1H). ^{13}C NMR (100 MHz, d_6-DMSO) δ: 109.72, 113.61, 122.57, 124.51, 125.23, 125.69, 126.14, 126.59, 129.79, 131.79, 132.37, 134.23, 136.78, 137.82, 161.18, 167.87. MS (ESI): $[M]^+$=375.31, $[M+2]^+$=377.29. Anal. calcd for $C_{16}H_{11}BrN_2O_2S$. C, 51.21; H, 2.95; N, 7.47; found: C, 50.96; H, 2.81; N, 7.30.

Compound 5(*E*)**.** Orange solid. Yield: 36%, mp 185-187 ºC. ^{1}H-NMR (400 MHz, d_6-DMSO) δ: 6.27 (d, *J*=2.8 Hz, 1H), 6.69 (d, *J*=2.8 Hz, 1H), 6.85 (d, *J*=8.4 Hz, 1H), 7.49 (dd, *J*=8.4 and 1.6 Hz, 1H), 7.56 (dd, *J*=5.2 and 1.2 Hz, 1H), 7.58 (s, 1H), 7.76 (m, 1H), 8.16 (m, 2H), 10.2 (s, 1H), 10.6 (s, 1H). ^{13}C NMR (100 MHz, d_6-DMSO) δ: 110.18, 116.38, 121.48, 122.94, 125.57, 126.05, 126.15, 127.99, 129.13, 130.20, 131.02, 132.53, 136.08, 139.71, 161.29, 169.65. MS (ESI): $[M]^+$=375.31, $[M+2]^+$=377.29. Anal. calcd for $C_{16}H_{11}BrN_2O_2S$. C, 51.21; H, 2.95; N, 7.47; found: C, 51.02; H, 2.77; N, 7.32.

*5.1.4.4. (Z)-2-Bromo-N-(3-((3-methylthiophen-2-yl)methylene)-2-oxoindolin-5-yl)acrylamide (**6**) and (E)-2-bromo-N-(3-((3-methylthiophen-2-yl)methylene)-2-oxoindolin-5-yl)acrylamide (**6**)*. Following general procedure C, after workup as described previously, the residue was purified by gradient flash chromatography on silica gel using EtOAc-light petroleum ether from 4:6 to 1:1 as eluent, affording compound **6**(*Z*) (EtOAc-light petroleum ether 4:6) and **6**(*E*) (EtOAc-light petroleum ether 1:1).

Compound 6(*Z*)**.** Yellow solid. Yield: 38%, mp 206-208 ºC. ^{1}H-NMR (400 MHz, d_6-DMSO) δ: 2.49 (s, 3H), 6.29 (d, *J*=3.2 Hz, 1H), 6.76 (d, *J*=3.2 Hz, 1H), 6.81 (d, *J*=8.0 Hz, 1H), 7.09 (d, *J*=5.2 Hz, 1H), 7.39 (dd, *J*=8.4 and 2.0 Hz, 1H), 7.79 (d, *J*=5.2 Hz, 1H), 7.82 (s, 1H), 7.92

(d, *J*=2.0 Hz, 1H), 10.1 (s, 1H), 10.6 (s, 1H). ^{13}C NMR (100 MHz, d_6-DMSO) δ: 15.14, 109.63, 113.57, 120.80, 122.34, 124.62, 125.07, 125.71, 126.17, 130.65, 131.33, 132.23, 133.13, 137.67, 146.46, 161.15, 167.93. MS (ESI): $[M]^+$=398.17, $[M+2]^+$=400.22. Anal. calcd for $C_{17}H_{13}BrN_2O_2S$. C, 52.45; H, 3.37; N, 7.20; found: C, 52.28; H, 3.18; N, 7.02.

Compound 6(*E*)**.** Orange solid. Yield: 33%, mp 189-191 ºC. ^{1}H-NMR (400 MHz, d_6-DMSO) δ: 2.42 (s, 3H), 6.28 (d, *J*=2.8 Hz, 1H), 6.72 (d, *J*=2.8 Hz, 1H), 6.86 (d, *J*=8.4 Hz, 1H), 7.18 (d, *J*=4.8 Hz, 1H), 7.44 (d, *J*=8.4 and 2.0 Hz, 1H), 7.76 (s, 1H), 7.95 (d, *J*=4.8 Hz, 1H), 8.62 (d, *J*=2.0 Hz, 1H), 10.3 (s, 1H), 10.6 (s, 1H). ^{13}C NMR (100 MHz, $CDCl_3$) δ: 15.07, 110.13, 116.94, 121.16, 122.96, 123.32, 125.60, 126.05, 126.14, 130.53, 131.15, 131.81, 132.53, 139.63, 145.38, 161.33, 169.86. MS (ESI): $[M]^+$=398.17, $[M+2]^+$=400.22. Anal. calcd for $C_{17}H_{13}BrN_2O_2S$. C, 52.45; H, 3.37; N, 7.20; found: C, 52.33; H, 3.22; N, 7.01.

5.1.4.5. (Z)-2-Bromo-N-(3-((5-methylthiophen-2-yl)methylene)-2-oxoindolin-5-yl)acrylamide (7) and (E)-2-bromo-N-(3-((5-methylthiophen-2-yl)methylene)-2-oxoindolin-5-yl)acrylamide (7). Following general procedure C, after workup as described previously, the residue was purified by gradient flash chromatography on silica gel using EtOAc-light petroleum ether from 4:6 to 1:1 as eluent, affording compound **7**(*Z*) (EtOAc-light petroleum ether 4:6) and **7**(*E*) (EtOAc-light petroleum ether 1:1).

Compound 7(*Z*)**.** Orange solid. Yield: 52%, mp 216-218 ºC. ^{1}H-NMR (400 MHz, d_6-DMSO) δ: 2.48 (s, 3H), 6.29 (d, *J*=3.2 Hz, 1H), 6.75 (d, *J*=3.2 Hz, 1H), 6.80 (d, *J*=8.0 Hz, 1H), 6.95 (dd, *J*=4.0 and 2.8 Hz, 1H), 7.27 (dd, *J*=8.0 and 2.0 Hz, 1H), 7.76 (d, *J*=4.0 Hz, 1H), 7.92 (m, 2H), 10.1 (s, 1H), 10.6 (s, 1H). ^{13}C NMR (100 MHz, $CDCl_3$) δ: 15.92, 109.66, 113.44, 120.46, 122.14, 124.95, 125.72, 126.10, 126.81, 129.36, 132.21, 135.83, 137.60, 139.39, 149.64, 161.14, 167.96. MS (ESI): $[M]^+$=398.31, $[M+2]^+$=400.20. Anal. calcd for $C_{17}H_{13}BrN_2O_2S$. C, 52.45; H, 3.37; N, 7.20; found: C, 52.29; H, 3.16; N, 6.98.

Compound 7(*E*)**.** Orange solid. Yield: 24%, mp 208-210 ºC. ^{1}H-NMR (400 MHz, d_6-DMSO) δ: 2.50 (s, 3H), 6.29 (d, *J*=2.8 Hz, 1H), 6.73 (d, *J*=2.8 Hz, 1H), 6.86 (d, *J*=8.0 Hz, 1H), 7.05

(dd, *J*=3.6 and 1.6 Hz, 1H), 7.48 (dd, *J*=8.0 and 2.0 Hz, 1H), 7.66 (d, *J*=3.6 Hz, 1H), 7.69 (s, 1H), 8.52 (d, J=2.0 Hz, 1H), 10.3 (s, 1H), 10.6 (s, 1H). ^{13}C NMR (100 MHz, d_6-DMSO) δ: 16.09, 110.09, 116.57, 121.29, 122.42, 122.79, 125.60, 126.05, 128.08, 128.34, 132.53, 135.62, 137.26, 139.46, 147.47, 161.39, 169.88. MS (ESI): $[M]^+$=398.31, $[M+2]^+$=400.20. Anal. calcd for $C_{17}H_{13}BrN_2O_2S$. C, 52.45; H, 3.37; N, 7.20; found: C, 52.33; H, 3.15; N, 7.03.

*5.1.4.6. 2-Bromo-N-(2-oxoindolin-5-yl)acrylamide (**19**).* Following general procedure C, after workup as described previously, the residue was purified by flash chromatography on silica gel using light petroleum ether: EtOAc 6:4 as eluent, affording compound **19** as a colour cream solid. Yield: 73%, mp 194-195 ºC. ^{1}H-NMR (400 MHz, d_6-DMSO) δ: 3.48 (s, 2H), 6.26 (d, *J*=2.8 Hz, 1H), 6.69 (d, *J*=2.8 Hz, 1H), 6.75 (d, *J*=8.4 Hz, 1H), 7.38 (d, *J*=8.4 Hz, 1H), 7.51 (s, 1H), 10.2 (s, 1H), 10.4 (s, 1H). ^{13}C NMR (100 MHz, d_6-DMSO) δ: 35.90, 108.72, 117.64, 119.97, 125.13, 125.35, 125.96, 132.08, 140.15, 160.61, 176.22. MS (ESI): $[M]^+$=281.3, $[M+2]^+$=283.3. Anal. calcd for $C_{11}H_9BrN_2O_2$. C, 47.00; H, 3.23; N, 9.97; found: C, 46.81; H, 3.15; N, 9.78.

5.2. Biological assays

5.2.1. Cell growth conditions and antiproliferative assay.

Human T-leukemia (CCRF-CEM and Jurkat) and human B-leukemia (RS4;11) and human promielocytic leukemia (HL-60) cells were grown in RPMI-1640 medium (Gibco, Milano, Italy). Breast adenocarcinoma (MCF-7), human cervix carcinoma (HeLa), and human colon adenocarcinoma (HT-29) cells were grown in DMEM medium (Gibco, Milano, Italy), all supplemented with 115 units/mL penicillin G (Gibco, Milano, Italy), 115 μg/mL streptomycin (Invitrogen, Milano, Italy), and 10% fetal bovine serum (Invitrogen, Milano, Italy). Stock solutions (10 mM) of the different compounds were obtained by dissolving them in DMSO. Individual wells of a 96-well tissue culture microtiter plate were inoculated with 100 μL of complete medium containing 8×10^3 cells. The plates were incubated at 37 °C in a humidified

5% CO_2 incubator overnigth prior to the experiments. After medium removal, 100 µL of fresh medium containing the test compound at different concentrations was added to each well in triplicate and incubated at 37 °C for 72 h. Cell viability was assayed by the (3-(4, 5-dimethylthiazol-2-yl)-2,5-diphenyltetrazolium bromide test as previously described [38]. Some experiments were also performed in the presence of DL-α-tocopherol acetate (TOC) or N-acetyl-L-cysteine (NAC), all purchased from Sigma-Aldrich (Milano, Italy).

Peripheral blood lymphocytes (PBL) from healthy donors were obtained from human peripheral blood (leucocyte rich plasma- buffy coats) from healthy volunteers using the Lymphoprep (Fresenius KABI Norge AS) gradient density centrifugation.

Buffy coats were obtained from the Blood Transfusion Service, Azienda Ospedaliera of Padova and provided at this institution for research purposes. Therefore, no informed consent was further needed. In addition, buffy coats were provided without identifiers. The experimental procedures were carried out in strict accordance with approved guidelines.

After extensive washing, cells were resuspended (1.0 x 10^6 cells/mL) in RPMI-1640 with 10% FBS and incubated overnight. For cytotoxicity evaluations in proliferating PBL cultures, non-adherent cells were resuspended at 5 x 10^5 cells/mL in growth medium, containing 2.5 μg/mL PHA (Irvine Scientific). Different concentrations of the test compounds were added, and viability was determined 72 h later by the MTT test. For cytotoxicity evaluations in resting PBL cultures, non-adherent cells were resuspended (5 x 10^5 cells/mL) and treated for 72 h with the test compounds, as described above.

5.2.2. Nek2 kinase activity assay.

Kinase assay was performed using the bioluminescent ADP-Glo™ kinase assay (Promega, Milano Italy), following manufacturer's instructions. Assay was performed with the test compounds at the final concentration of 1 µM.

5.2.3. Flow Cytometric Analysis of Cell Cycle Distribution.

5×10^5 HeLa or Jurkat cells were treated with different concentrations of the test compounds for 24 h. After the incubation period, the cells were collected, centrifuged, and fixed with ice-cold ethanol (70%). The cells were then treated with lysis buffer containing RNase A and 0.1% Triton X-100 and then stained with PI. Samples were analyzed on a Cytomic FC500 flow cytometer (Beckman Coulter). DNA histograms were analyzed using MultiCycle for Windows (Phoenix Flow Systems).

5.2.4. Apoptosis Assay.

Cell death was determined by flow cytometry of cells double stained with annexin V/FITC and PI. The Coulter Cytomics FC500 (Beckman Coulter) was used to measure the surface exposure of PS on apoptotic cells according to the manufacturer's instructions (Annexin-V Fluos, Roche Diagnostics).

5.2.5. Western Blot Analysis.

HeLa cells were incubated in the presence of test compounds and after different times, were collected, centrifuged, and washed two times with ice cold phosphate buffered saline (PBS). The pellet was then resuspended in lysis buffer. After the cells were lysed on ice for 30 min, lysates were centrifuged at 15000 x g at 4 °C for 10 min. The protein concentration in the supernatant was determined using the BCA protein assay reagents (Pierce, Italy). Equal amounts of protein (10 μg) were resolved using sodium dodecyl sulfate-polyacrylamide gel electrophoresis (SDS-PAGE) (7.5−15% acrylamide gels) and transferred to Immobilon-P membrane (Millipore, Milano, Italy). Membranes were blocked with a bovine serum albumin (BSA) solution (BSA 3%, Tween 0.1% in PBS), the membranes being gently rotated for two hours at room temperature. Membranes were then incubated overnight at 4 °C with primary antibodies against caspase-9, and γH2AX (Cell Signaling), or β-actin (Sigma-Aldrich) for 2 h at room temperature. Membranes were next incubated with peroxidase labeled secondary

antibodies for 60 min. All membranes were visualized using ECL Select (GE Healthcare) and images were acquired using an Uvitec-Alliance imaging system (Uvitec, Cambridge, UK). To ensure equal protein loading, each membrane was stripped and reprobed with anti-β-actin antibody. Quantitative analysis of western blot was performed by Image J software and the results were normalized to β-actin.

5.2.6. Assessment of mitochondrial changes and ROS production.

The mitochondrial membrane potential was measured with the lipophilic cation JC-1 (Molecular Probes, Eugene, OR, USA), while the production of ROS was followed by flow cytometry using the fluorescent dye H_2DCFDA (Molecular Probes), as previously described[39].

5.2.7. Detection of the intracellular GSH content.

Cellular GSH levels were analyzed using CMFDA (Molecular Probes) [40]. Cells were treated with the test compound for different times. Cells were harvested, centrifuged and incubated in the presence of a solution of 5 μM CMFDA at 37 °C for 30 min. Cytoplasmic esterases convert non-fluorescent CMFDA to fluorescent 6-chloromethylfluorescein, which can then react with GSH. Fluorescence intensity was determined by flow cytometry.

Acknowledgments.

The authors gratefully acknowledged Alberto Casolari for the excellent technical assistance.

Supplementary data. Spectra of compounds **3-7**. Supplementary data associated with this article can be found in the online version**.**

References

[1] M. Kaur, M. Singh, N. Chadha, O. Silakari. Oxindole: A chemical prism carrying plethora of therapeutic benefits. Eur. J. Med. Chem. 123 (2016) 858-894.

[2] L. Sun L, N. Tran, C. Liang, F. Tang, A. Rice, R. Schreck, K. Waltz, L.K. Shawver, G. McMahon, C. Tang. Design, synthesis, and evaluations of substituted 3-[(3- or 4-carboxyethylpyrrol-2-yl)methylidenyl]indolin-2-ones as inhibitors of VEGF, FGF, and PDGF receptor tyrosine kinases. J. Med. Chem. 42 (1999) 5120-5130.

[3] L. Mologni, R. Rostagno, S. Brussolo, P.P. Knowles, S. Kjaer, J. Murray-Rust, E. Rosso, A. Zambon, L. Scapozza, N.Q. McDonald, V. Lucchini, C. Gambacorti-Passerini. Synthesis, structure-activity relationship and crystallographic studies of 3-substituted indolin-2-one RET inhibitors. Bioorg. Med. Chem. 18 (2010) 1482-1496.

[4] A. Nagarsenkar, L. Guntuku, S. D. Guggilapu, DB K., S. Gannoju, V.G. Naidu, N. B. Bathini. Synthesis and apoptosis inducing studies of triazole linked 3-benzylidene isatin derivatives, Eur. J. Med. Chem. 124 (2016) 782-793.

[5] A. Kamal, A.B, Shaik, N. Jain, C. Kishor, A. Nagabhushana, B. Supriya, G. Bharath Kumar, S.S. Chourasiya, Y. Suresh, R.K. Mishra, A. Addlagatta. Design and synthesis of pyrazole-oxindole conjugates targeting tubulin polymerization as new anticancer agents. Eur. J. Med. Chem. 92 (2015) 501-513.

[6] G.H. Zheng, J.J.Shen, Y.C. Zhan, H. Yi, S.T.Xue, Z, Wang, X.Y. Ji, Z.R. Li. Design, synthesis and in vitro and in vivo antitumour activity of 3-benzylideneindolin-2-one derivatives, a novel class of small-molecule inhibitors of the MDM2-p53 interaction. Eur. J. Med. Chem. 81 (2014) 277-288.

[7] S. Sestito, S. Daniele, G. Nesi, E. Zappelli, S. Rapposelli. Locking PDK1 in DFG-out conformation through 2-oxo-indole containing molecules: Another tools to fight glioblastoma. Eur. J. Med. Chem. 118 (2016) 47-63.

[8] G. Chen, Q. Weng, L. Fu, Z. Wang, P. Yu, Z. Liu, X. Li, H. Zhang, G. Liang. Synthesis and biological evaluation of novel oxindole-based RTK inhibitors as anti-cancer agents. Bioorg. Med. Chem. 22 (2014) 6953-6960.

[9] L. Sun, N. Tran, F. Tang, H. App, G. McMahon, C. Tang C. Synthesis and biological evaluations of 3-substituted indolin-2-ones: a novel class of tyrosine kinase inhibitors that exhibit selectivity toward particular receptor tyrosine kinases. J, Med. Chem. 41 (1998) 2588-2603.

[10] J. Tammiku-Taul, R. Park, K. Jaanson, K. Luberg, M. Karelson. Indole-like Trk receptor antagonists. Eur. J. Med. Chem. 121 (2016) 541-552.

[11] R Roskoski Jr. Sunitinib: a VEGF and PDGF receptor protein kinase and angiogenesis inhibitor. Biochem. Biophys. Res. Commun. 356 (2007) 323-328.

[12] J. Dancey, E.A. Sausville. Issues and progress with protein kinase inhibitors for cancer treatment. Nat Rev Drug Discov. 2 (2003) 296-313.

[13] a) J.C. Henise, J. Taunton. Irreversible Nek2 kinase inhibitors with cellular activity. J. Med. Chem. 54 (2011) 4133-4146; b) P. Rellos, F.J. Ivins, J.E. Baxter, A. Pike, T.J. Nott, D.-M. Parkinson, S. Das, S. Howell, O. Fedorov, Q.Y. Shen, A.M. Fry, S. Knapp, S.J. Smerdon. Structure and regulation of the human Nek2 centrosomal kinase. J. Biol. Chem. 282 (2006) 6833-6842.

[14] G. Nesi, S. Sestito, V. Mey, S. Ricciardi, M. Falasca, R. Danesi, A. Lapucci, M.C. Breschi, S. Fogli, S. Rapposelli. Synthesis of novel 3,5-disubstituted-2-oxindole derivatives as antitumor agents against human nonsmall cell lung cancer. ACS Med Chem Lett. 4 (2013) 1137-1141.

[15] R. Romagnoli, P. G. Baraldi, O. Cruz-Lopez, C. Lopez-Cara, D. Preti. α-Halogenoacrylic derivatives of antitumor agents. Mini-Rev. Med. Chem. 9 (2009) 81-94.

[16] D. Lorusso, S. Mainenti, A. Pietragalla, G. Ferrandina, G. Foco, V. Masciullo, G. Scambia, Brostallicin (PNU-166196), a new minor groove DNA binder: preclinical and clinical activity. Expert Opin. Invest. Drugs. 18 (2009**)** 1939-1946.

[17] M. Leahy, I. Ray-Coquard, J. Verwei, A. Le Cesne, F. Duffaud, P. C. Hogendoorn, C. Fowst, C. De Balincourt, E. D. Di Paola, M. Van Glabbeke, I. Judson, J. Y. Blay, Brostallicin, an agent with potential activity in metastatic soft tissue sarcoma: a phase II study from the European Organisation for Research and Treatment of Cancer Soft Tissue and Bone Sarcoma Group. Eur. J. Cancer 43 (2007) 308-315.

[18] A. Ali, S. Bhattachary, DNA binders in clinical trials and chemotherapy. Bioorg. Med. Chem. 22 (2014) 4506-4521.

[19] I. Beria, P.G. Baraldi, P. Cozzi, M. Caldarelli, C. Geroni, S. Marchini, N. Mongelli, R. Romagnoli, Cytotoxic alpha-halogenoacrylic derivatives of distamycin A and congeners. J. Med. Chem. 47 (2004) 2611-2613.

[20] J. Singh, R.C. Petter, A.F.; Targeted covalent drugs of the kinase family. Curr. Opin. Chem. Biol. 14 (2010) 475-480.

[21] S. Sestito, G. Nesi, S. Daniele, A. Martelli, M. Digiacomo, A. Borghini, D. Pietra, V. Calderone, A. Lapucci, M. Falasca, P. Parrella, A. Notarangelo, M.C. Breschi, M. Macchia, C. Martini , S. Rapposelli. Design and synthesis of 2-oxindole based multi-targeted inhibitors of PDK1/Akt signaling pathway for the treatment of glioblastoma multiforme. Eur. J. Med. Chem. 105 (2015) 274-288.

[22] A. Millemaggi, R. J. K. Taylor. 3-Alkenyl-oxindoles: natural products, pharmaceuticals, and recent synthetic advances in tandem/telescoped approaches. Eur. J. Org. Chem. 24 (2010) 4527-4547.

[23] M. H. Ngai, C. L. So, M. B. Sullivan, H. K. Ho, C. L. L. Chai. Photoinduced isomerization and hepatoxicities of Semaxanib, Sunitinib and related 3-substituted indolin-2-ones. ChemMedChem 11 (2016) 72-80.

[24] L. Sun, C. Liang, S. Shirazian, Y. Zhou, T. Miller, J. Cui, J. Y. Fukuda, J.-Y. Chu, A. Nematalla, X. Wang, H. Chen, A. Sistla, T. C. Luu, F. Tang, J. Wei, C. Tang. Discovery of 5-[5-fluoro-2-oxo-1,2-dihydroindol-(3Z)-ylidenemethyl]-2,4-dimethyl-

1*H*-pyrrole-3-carboxylic acid (2-diethylaminoethyl)amide, a novel tyrosine kinase inhibitor targeting vascular endothelial and platelet-derived growth factor receptor tyrosine kinase. J. Med. Chem. 46 (2003) 1116-1119.

[25] J.D. Ly, D.R. Grubb, A. Lawen. The mitochondrial membrane potential (deltapsi(m)) in apoptosis; an update. Apoptosis. 8 (2003) 115-128.

[26] P.D. Bhola, A.Letai. Mitochondria-judges and executioners of cell death sentences. Mol Cell. 61 (2016) 695-704.

[27] E. Lugli, L. Troiano, A. Cossarizza Polychromatic analysis of mitochondrial membrane potential using JC-1. Curr Protoc Cytom. 2007 Jul;Chapter 7:Unit 7.32.

[28] M.L. Würstle, M.A. Laussmann, M. Rehm The central role of initiator caspase-9 in apoptosis signal transduction and the regulation of its activation and activity on the apoptosome. Exp Cell Res. 318 (2012) 1213-1220.

[29] A. Cossarizza. R. Ferraresi, L. Troiano, E. Roat, L. Gibellini, L. Bertoncelli, M. Nasi, M. Pinti. Simultaneous analysis of reactive oxygen species and reduced glutathione content in living cells by polychromatic flow cytometry. Nature Protocols 4 (2009) 1790-1797.

[30] J. Cai, D.P. Jones Superoxide in apoptosis. Mitochondrial generation triggered by cytochrome c loss. J. Biol. Chem. 273 (1998) 11401-11404.

[31] N. Zamzami, P. Marchetti, M. Castedo, D. Decaudin, A. Macho, T. Hirsch, S.A. Susin, P.X. Petit, B. Mignotte, Kroemer, G. Sequential reduction of mitochondrial transmembrane potential and generation of reactive oxygen species in early programmed cell death. J. Exp. Med. 182 (1995) 367-377.

[32] R. Romagnoli, P.G. Baraldi, M.K. Salvador, M. Chayah, M.E. Camacho, F. Prencipe, E. Hamel, F. Consolaro, G. Basso, G. Viola. Design, synthesis and biological evaluation of arylcinnamide hybrid derivatives as novel anticancer agents. Eur J Med Chem. 81 (2014) 394-407.

[33] I. Mostafa Fekry, N. E. Price, H. Zang, C. Huang, M. Harmata, P.Brown, J. Scott Daniels, K. S. Gates. Thiol-activated DNA damage by α-bromo-2-cyclopentenone. Chem Res Toxicol 24 (2011) 217-228.

[34] D.W Hedley, S. Chow. Evaluation of methods for measuring cellular glutathione content using flow cytometry. Cytometry 15 (1994) 349-358.

[35] M. L. Circu, Aw, T. Y. Glutathione and apoptosis. Free Radic. Res. 42 (2008) 689-706.

[36] O. Fernandez-Capetillo, A. Lee, M. Nussenzweig, A. Nussenzweig. H2AX: the histone guardian of the genome. DNA Repair 3 (2004) 959-967.

[37] D. Trachootham, J. Alexandre, P. Huang Targeting cancer cells by ROS-mediated mechanisms: A radical therapeutic approach? Nat. Rev. Drug Discov. 8 (2009) 579-591.

[38] R. Romagnoli, P.G. Baraldi, C. Lopez-Cara, M. Kimatrai Salvador, D. Preti, M. Aghazadeh Tabrizi, M. Bassetto, A. Brancale, E. Hamel, I. Castagliuolo, R. Bortolozzi, G. Basso., G. Viola Synthesis and biological evaluation of 2-alkoxycarbonyl-3-anilino benzo[*b*]thiophenes and thieno[2,3-*b*]pyridines as new potent anticancer agents. J. Med. Chem. 56 (2013) 2606-2618.

[39] G. Viola, E. Fortunato, L. Cecconet, L. Del Giudice, F. Dall'Acqua, G. Basso Central role of mitochondria and p53 in PUVA-induced apoptosis in human keratinocytes cell line NCTC-2544. Toxicol Appl Pharmacol 227 (2008) 84-96.

[40] G. Viola, P. Grobelny P., M.A. Linardi, A. Salvador, G. Basso, J. Mielcarek, S. Dall'Acqua, D. Vedaldi, F. Dall'Acqua The phototoxicity of fluvastatin an HMG-CoA reductase inhibitor is mediated by the formation of a benzocarbazol-like photoproduct. Toxicol. Sci. 118 (2010) 236-250.

Table 1. *In vitro* cell growth inhibitory effects of compounds **3-7**, **19** and **1e**

Compd	IC_{50} [a](nM)						
	HL-60	Jurkat	CCRF-CEM	RS4;11	HeLa	HT-29	MCF-7
3(*Z*)	140±60	110±50	3±1	1±0.4	500±200	800±200	700±100
4(*Z*)	230±90	210±90	35±1	2±1	1700±400	240±80	1700±600
4(*E*)	15±6	16±7	10±5	30±10	1800±500	5500±1100	2300±150
5(*Z*)	350±20	190±30	4±1	190±10	3500±900	600±60	2800±400
5(*E*)	770±240	56±9	6±0.6	190±8	2600±110	310±80	2100±120
6(*Z*)	13±5	30±4	0.5±0.1	0.4±0.09	420±100	1200±600	2600±1000
6(*E*)	39±3	40±10	0.9±0.5	4±1	450±200	330±80	2300±1000
7(*Z*)	24±6	360±160	9±4	50±20	1600±600	560±50	3000±700
7(*E*)	12±7	150±60	1±0.5	20±10	2000±800	300±100	4400±600
19	350±9	1100±330	220±20	220±07	4500±500	4400±600	3300±1300
1e	5800±700	340±60	50±10	70±20	4400±200	2300±60	3700±100

[a]IC_{50}= compound concentration required to inhibit tumor cell proliferation by 50%. Data are expressed as the mean ± SE from the dose-response curves of at least three independent experiments carried out in triplicate.

Table 2. Cytotoxicity of **3**(*Z*) and **6**(*E*) for human peripheral blood lymphocytes (PBL)

	IC_{50} (μM) [a]	
	3(*Z*)	**6**(*E*)
$PBL_{resting}$ [b]	1.5±0.39	0.45±0.068
PBL_{PHA} [c]	0.83±0.04	1.22±0.35

[a] Compound concentration required to reduce cell growth inhibition by 50%.
[b] PBL not stimulated with PHA.
[c] PBL stimulated with PHA.
Values are the mean ± SEM for two separate experiments.

Figure Legends

Chart 1. Structure of 3,5-disubstituted-2-oxindole derivatives **1a-f** and PNU-166196 or Brostallicin (**2**).

Chart 1. Structure of 5-α-bromoacryloylamido-3-substituted-2-oxindole hybrid derivatives **3-7.**

Scheme 1. **Reagents**: **a**: Appropriate aldehyde, piperidine (cat.), DMF, 80 °C, 3 h; **b**: Fe, NH_4Cl, EtOH-water, reflux, 2h; **c**: α-bromoacrylic acid, EDCI, HOBt, DMF, rt, 18 h.

Figure 1. Panel A. Inhibition of Nek2 enzymatic activity by test compounds at the concentration of 1 μM. Data are represented as means ± SEM of two independent experiments performed in duplicate. Panel B. Percentage of cells in each phase of the cell cycle in HeLa cells treated with compounds **3**(*Z*), **6**(*E*) and **1e** at the indicated concentrations for 24 h. Cells were fixed and labeled with PI and analyzed by flow cytometry as described in the experimental section.

Figure 2. Flow cytometric analysis of apoptotic cells after treatment of HeLa (Panels A and B) and Jurkat cells (Panels C and D) with compounds **3**(*Z*) and **6**(*E*) at the indicated concentrations after incubation for 24 (Panels A and C) or 48 h (Panels B and D). The cells were harvested and labeled with annexin-V-FITC and PI and analyzed by flow cytometry. Data are represented as means ± SEM of three independent experiments.

Figure 3. Assessment of mitochondrial membrane potential ($\Delta\psi_{mt}$) following treatment of HeLa cells (Panel A) and Jurkat cells (Panel B) with compounds **3**(*Z*) and **6**(*E*) at the indicated concentrations. Cells were stained with JC-1 at the indicated times and analyzed by flow cytometry to measure dissipation of mitochondrial potential. Panel C. Representative western blot analysis of caspase-9 expression in HeLa cells after 24 h of treatment with the

indicated compounds at the indicated concentrations. Panel D. Quantification of western blot was performed by ImageJ software. Data are expressed as mean±SD of two different gels.

Figure 4. ROS production in Hela (Panel A) and Jurkat cells (Panel B). Cells were treated with **3**(*E*) and **6**(*Z*) and at the indicated times stained with H_2DCFDA and analyzed by flow cytometry to measure ROS production. Compounds **3**(*E*) and **6**(*Z*) induced GSH depletion in HeLa (Panel C) and Jurkat cells (Panel D). Cells were treated with the indicated concentration of compounds and after 12-24 h incubations, the cells were stained with the fluorescent probe CMFDA and analyzed by flow cytometry. Data represent means ± S.E.M. of three independent experiments.

Figure 5. A. Effect of ROS scavengers on cell death induced by compounds **3**(*Z*) and **6**(*E*). HeLa cells were treated with the two compounds at 1.0 μM for 48 h in the presence of NAC (100 μM) and TOC (100 μM). Cell viability was measured by Annexin-V assay. Data are represented as means ± S.E.M. for three independent experiments. *$p<0.05$ vs compound alone. B. Representative western blot analysis of γH2A.X expression in HeLa cells after treatment for 24 h with **3**(*Z*) and **6**(*E*) at the indicated concentrations. C. Quantification of western blots was performed by ImageJ software. Data are expressed as mean±SD of two different gels.

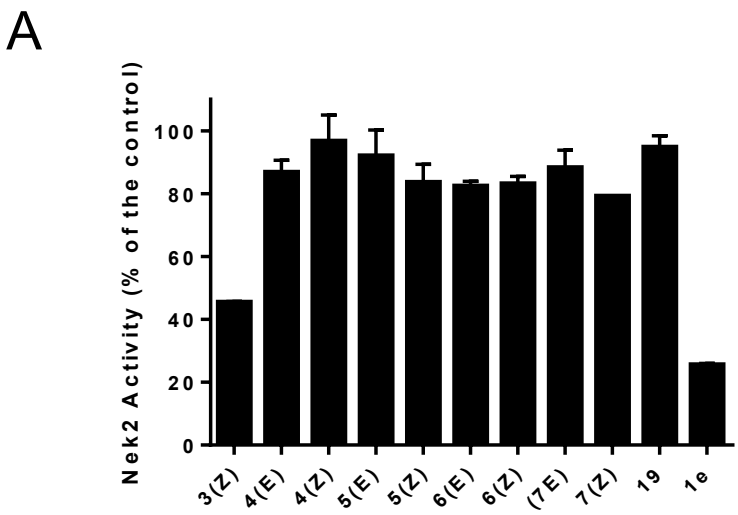
A
Nek2 Activity (% of the control)
0
20
40
60
80
100
3(Z)
4(E)
4(Z)
5(E)
5(Z)
6(E)
6(Z)
(7E)
7(Z)
19
1e

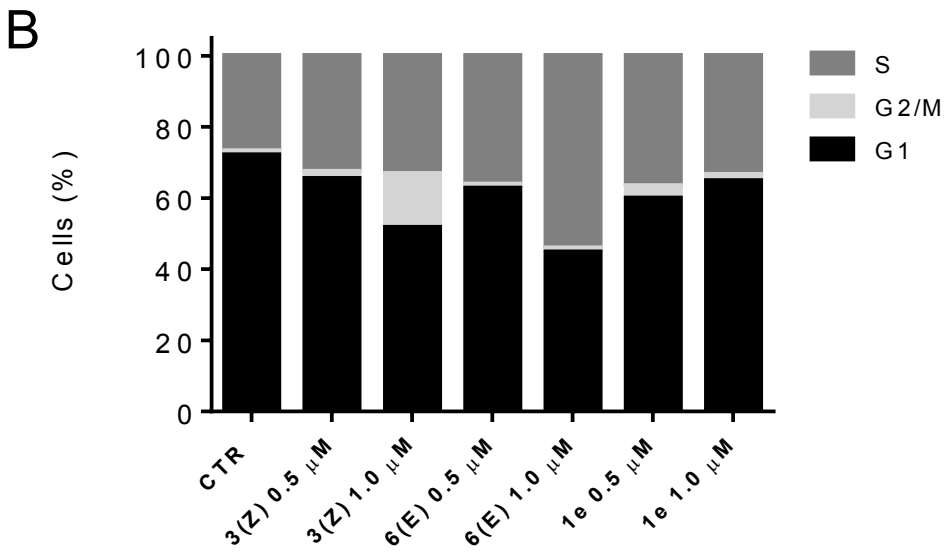
B
Cells (%)
0
20
40
60
80
100
CTR
3(Z) 0.5 μM
3(Z) 1.0 μM
6(E) 0.5 μM
6(E) 1.0 μM
1e 0.5 μM
1e 1.0 μM
S
G2/M
G1

Figure 1

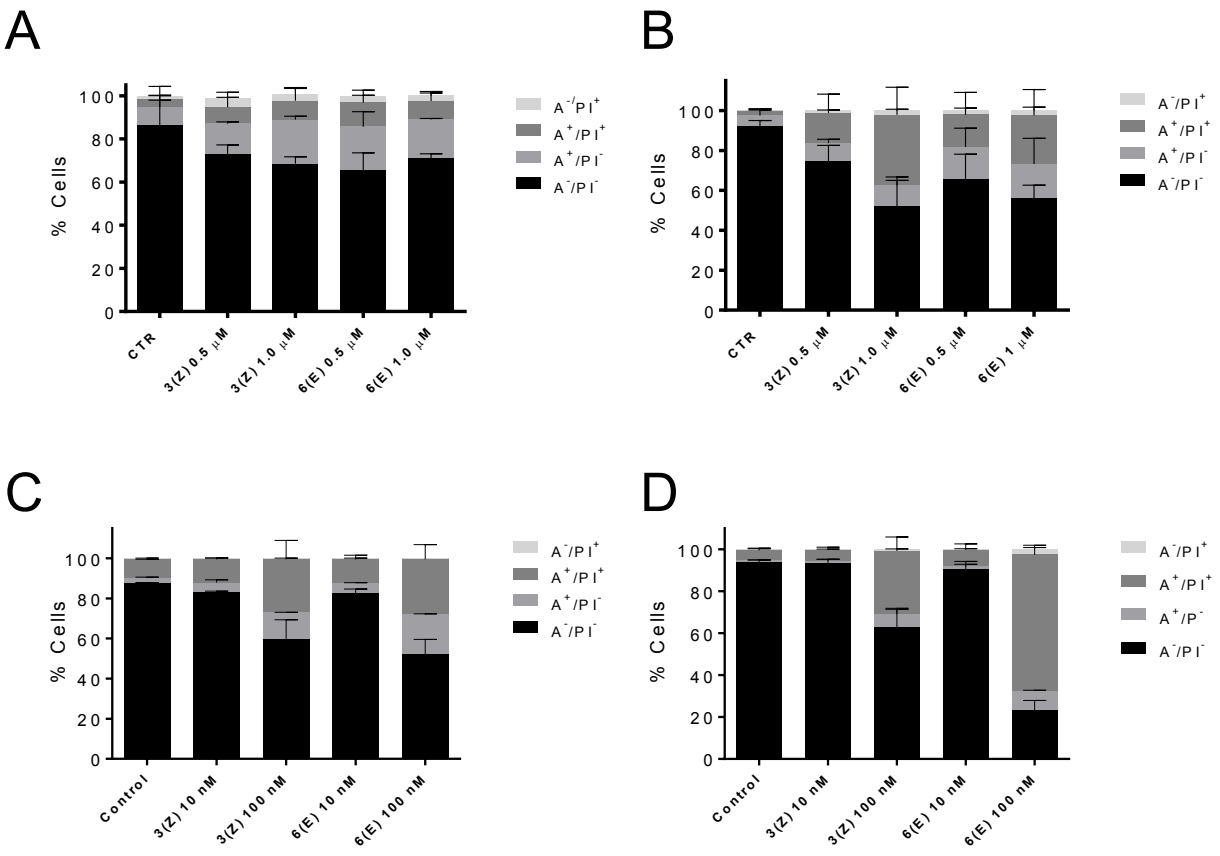
A
B
C
D
% Cells
CTR
3(Z) 0.5 μM
3(Z) 1.0 μM
6(E) 0.5 μM
6(E) 1.0 μM
3(Z) 1 μM
6(E) 1 μM
Control
3(Z) 10 nM
3(Z) 100 nM
6(E) 10 nM
6(E) 100 nM
A-/PI+
A+/PI+
A+/PI-
A-/PI-
A+/P-

Figure 2

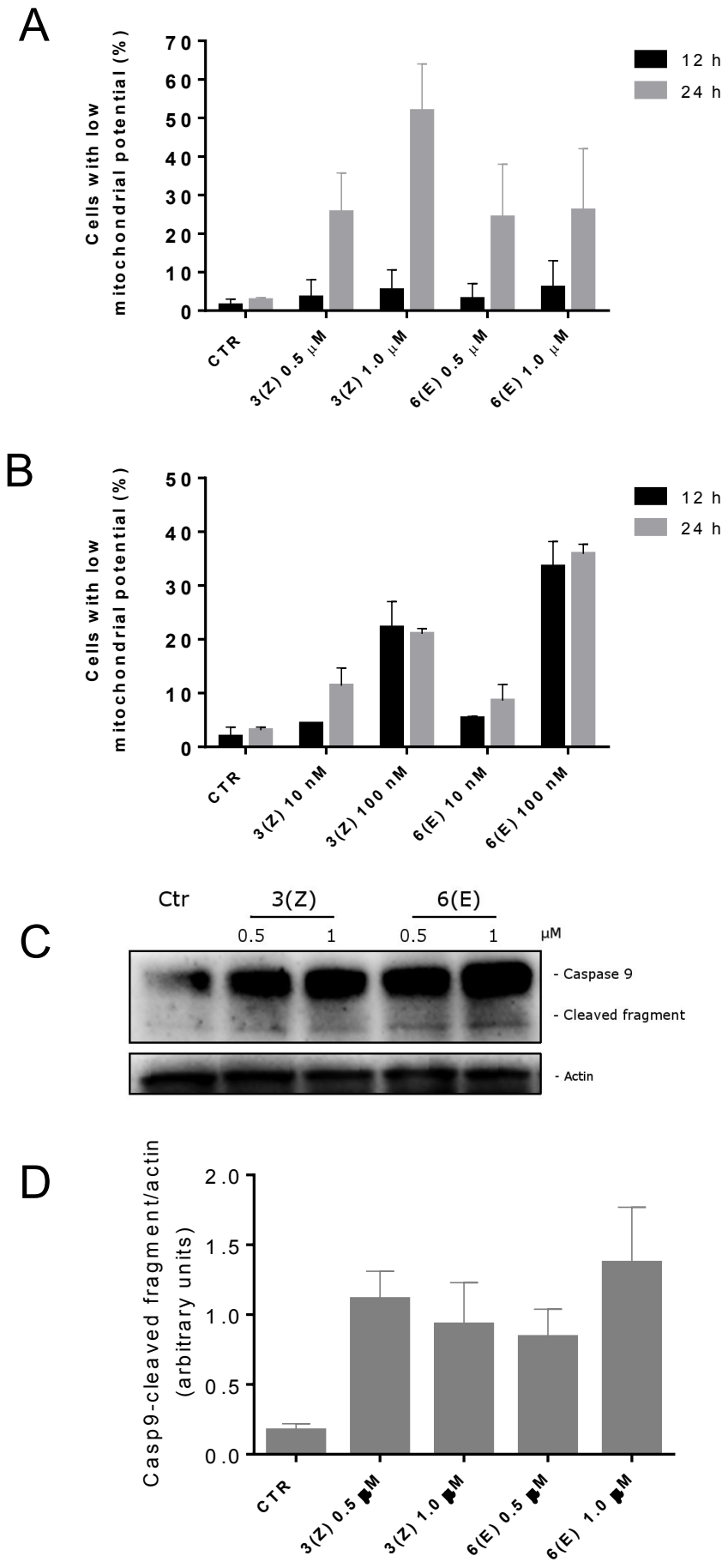
A
Cells with low mitochondrial potential (%)
70
60
50
40
30
20
10
0
12 h
24 h
CTR
3(Z) 0.5 μM
3(Z) 1.0 μM
6(E) 0.5 μM
6(E) 1.0 μM
B
Cells with low mitochondrial potential (%)
50
40
30
20
10
0
12 h
24 h
CTR
3(Z) 10 nM
3(Z) 100 nM
6(E) 10 nM
6(E) 100 nM
C
Ctr
3(Z)
6(E)
0.5
1
0.5
1
μM
- Caspase 9
- Cleaved fragment
- Actin
D
Casp9-cleaved fragment/actin (arbitrary units)
2.0
1.5
1.0
0.5
0.0
CTR
3(Z) 0.5 μM
3(Z) 1.0 μM
6(E) 0.5 μM
6(E) 1.0 μM

Figure 3

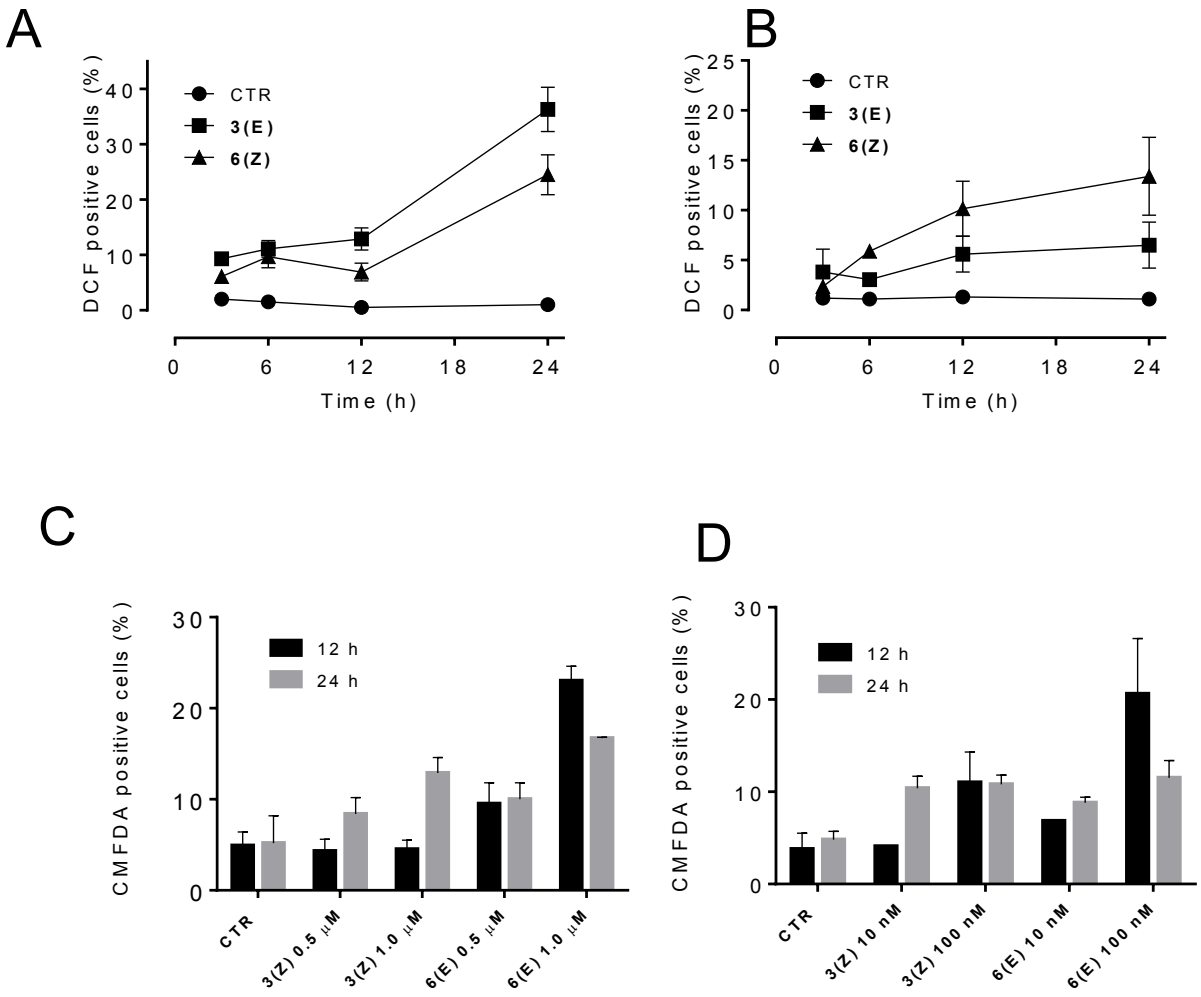
A
DCF positive cells (%)
CTR
3(E)
6(Z)
Time (h)
B
DCF positive cells (%)
CTR
3(E)
6(Z)
Time (h)
C
CMFDA positive cells (%)
12 h
24 h
CTR
3(Z) 0.5 μM
3(Z) 1.0 μM
6(E) 0.5 μM
6(E) 1.0 μM
D
CMFDA positive cells (%)
12 h
24 h
CTR
3(Z) 10 nM
3(Z) 100 nM
6(E) 10 nM
6(E) 100 nM

Figure 4

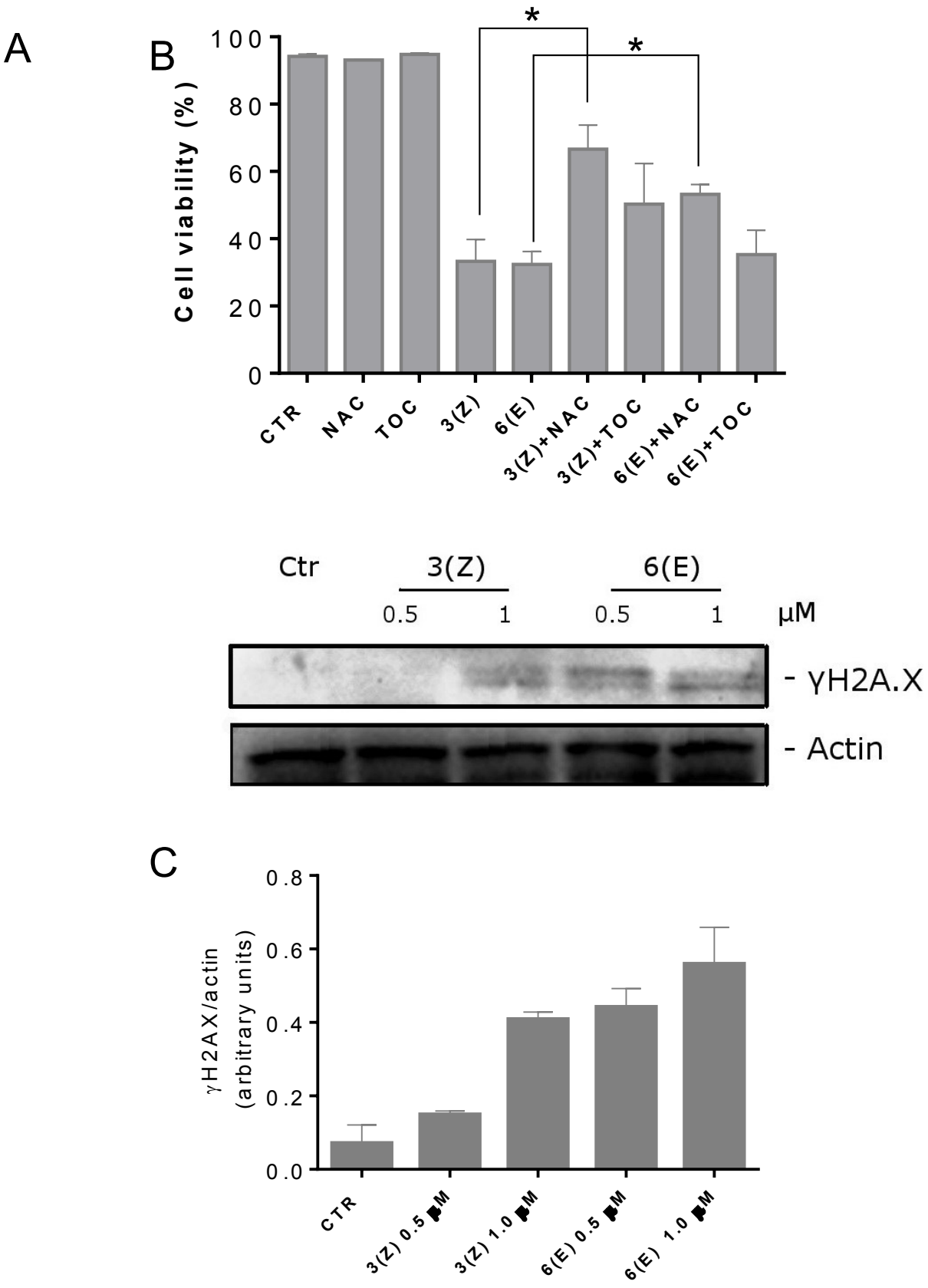
A
B
Cell viability (%)
100
80
60
40
20
0
*
*
CTR
NAC
TOC
3(Z)
6(E)
3(Z)+NAC
3(Z)+TOC
6(E)+NAC
6(E)+TOC
Ctr
3(Z)
6(E)
0.5
1
0.5
1
μM
- γH2A.X
- Actin
C
γH2AX/actin
(arbitrary units)
0.8
0.6
0.4
0.2
0.0
CTR
3(Z) 0.5 μM
3(Z) 1.0 μM
6(E) 0.5 μM
6(E) 1.0 μM

Figure 5

Chart 1.

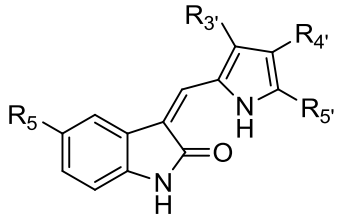

SU 5402 (**1a**), $R_{3'}=(CH_2)_2CO_2H$, $R_{4'}=CH_3$, $R_{5'}=R_5=H$
SU 5416 (**1b**), $R_{3'}=R_{5'}=CH_3$, $R_{4'}=R_5=H$
SU 6668 (**1c**), $R_{3'}=R_{5'}=CH_3$, $R_{4'}=(CH_2)_2CO_2H$, $R_5=H$
Sunitinib (**1d**), $R_{3'}=R_{5'}=CH_3$, $R_{4'}=(C_2H_5)N(CH_2)_2NHCO$, $R_5=F$

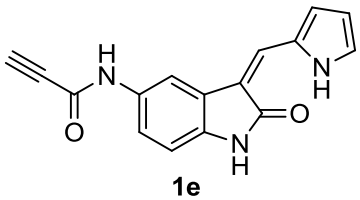

1e

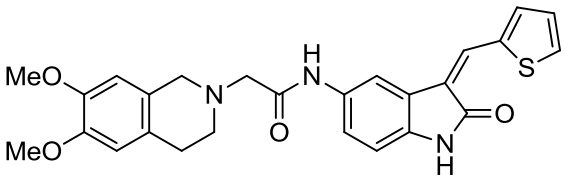

1f

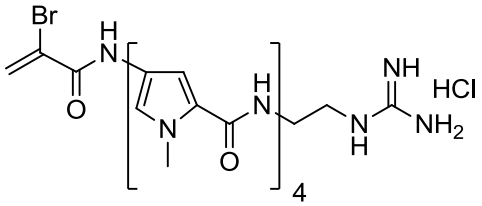

PNU-166196 or Brostallicin (**2**)

Chart 2

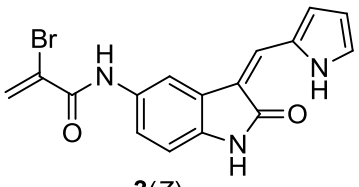

3(*Z*)

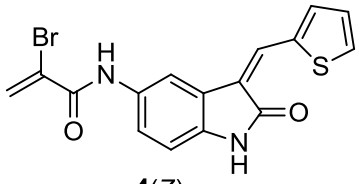

4(*Z*)

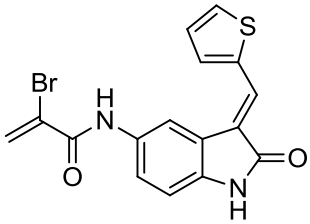

4(*E*)

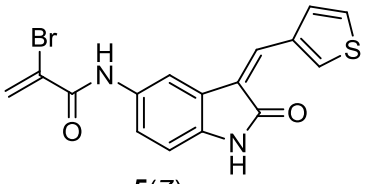

5(*Z*)

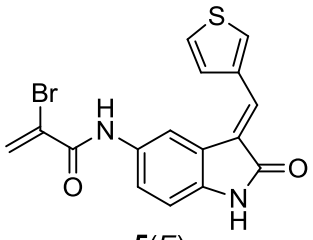

5(*E*)

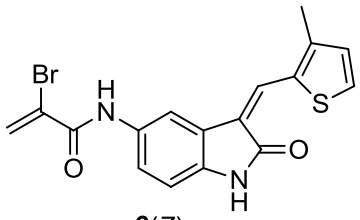

6(*Z*)

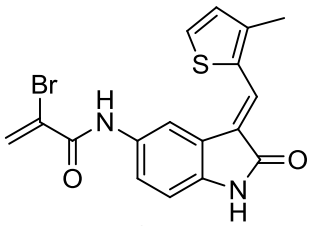

6(*E*)

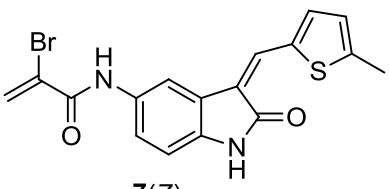

7(*Z*)

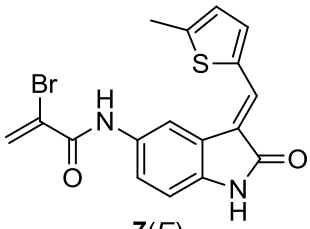

7(*E*)

Scheme 1

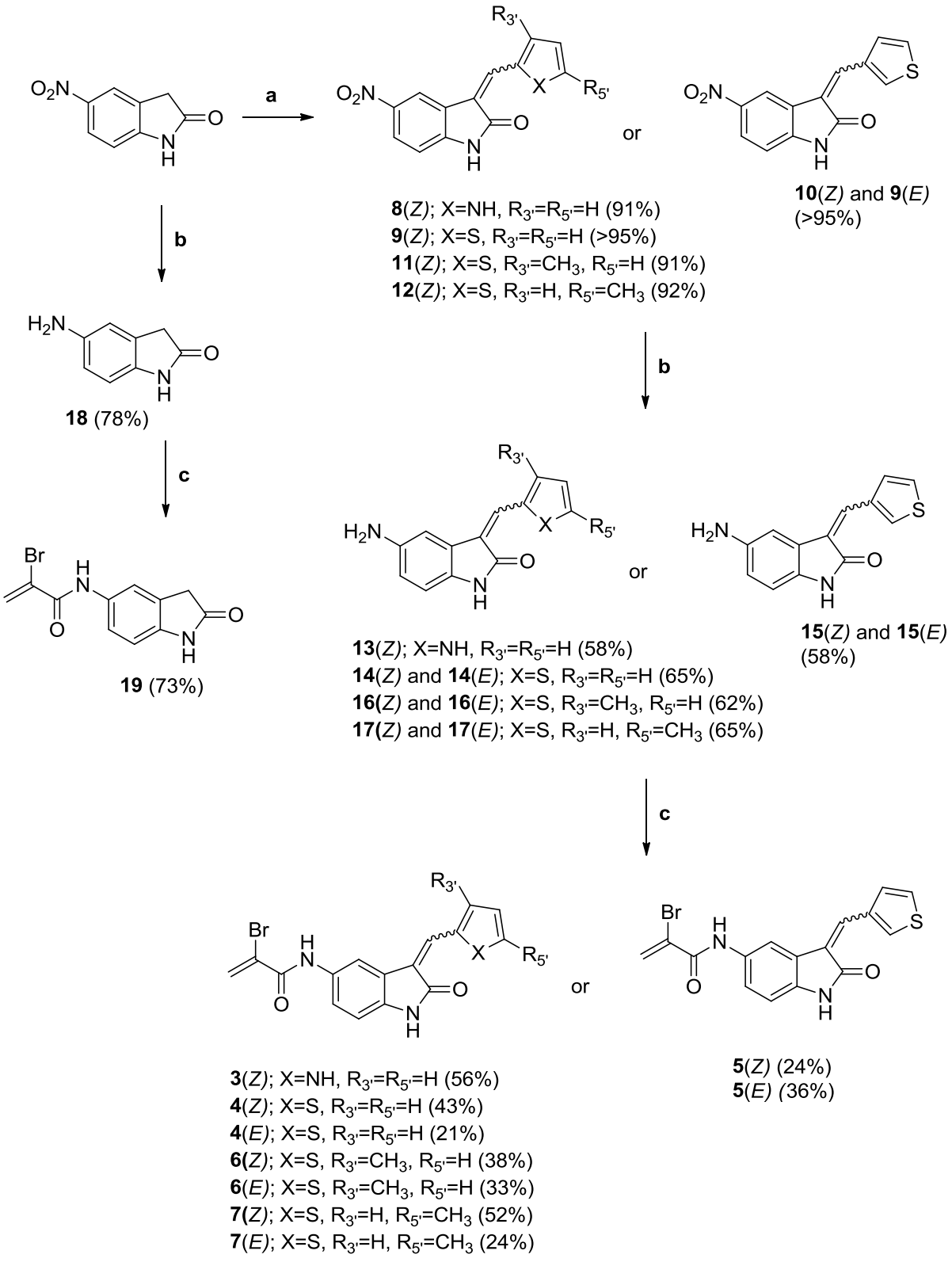

Scheme 1. **Reagents**: **a**: Appropriate aldehyde, piperidine (cat.), DMF, 80 °C, 3 h; **b**: Fe, NH_4Cl, EtOH-water, reflux, 2h; **c**: α-bromoacrylic acid, EDCI, HOBt, DMF, rt, 18 h.